Optimal Control of Li-Ion Hydrogen Fuel Cell Hybrid Vehicles

by

Michael Karpinski-Leydier

A thesis
presented to the University of Waterloo
in fulfillment of the
thesis requirement for the degree of
Master of Applied Science
in
Mechanical Engineering

Waterloo, Ontario, Canada, 2012

I hereby declare that I am the sole author of this thesis. This is a true copy of the thesis, including any required final revisions, as accepted by my examiners.

I understand that my thesis may be made electronically available to the public.

Abstract

Hydrogen fuel cells are poised to become the next major power generation technology for the automotive industry. In order to make fuel cell powered vehicles viable for every day use, it is necessary to study how to control these vehicles to minimize fuel consumption, thus reducing operation costs and increasing the vehicle's range. Although hybrid vehicle control strategies have been extensively studied, there is relatively little existing research into fuel cell hybrid vehicle control.

Fuel cell hybrid vehicles have similar power trains to conventional series hybrid electric vehicles where the engine and generator are replaced with a fuel cell and a DC/DC converter. The underlying hybrid control concepts used for conventional hybrid vehicles are still valid although it is unknown how well they will perform on fuel cell based vehicles since the fuel cell is a fundamentally different power source.

This thesis reviews several control strategies for fuel cell vehicles including a mode switching rule-based control strategy, a constant fuel cell output strategy and an adaptive variation of the equivalent consumption minimization strategy (A-ECMS) which has been modified for fuel cell vehicles. These strategies are implemented in simulation and evaluated against optimal strategies. The optimal strategies have been determined using convex optimization problem solving techniques that have been adapted to a fuel cell specific version of the hybrid vehicle control problem.

The mode switching and constant fuel cell strategies have also been evaluated in real world testing on a fully functional, road safe, fuel cell powered SUV. The test vehicle was designed and built by the University of Waterloo Alternative Fuels Team (UWAFT) for the EcoCAR competition. My responsibilities on the team were primarily to develop the rear motor and hybrid control logic as well as to assist in the testing and physical construction of the vehicle.

The simulation results demonstrate that near optimal fuel economies can be achieved through operating the fuel cell at near peak efficiency while the battery manages all major transients in the power demand. The constant fuel cell strategy demonstrates the highest fuel economy of all the tested strategies since it operates continually within this high efficiency region. The mode based strategy showed the worst results since the fuel cell would follow the transients of the power demand, pushing it out of the peak efficiency region. These results were validated by the experimental results which showed similar relationships between the mode switching, constant fuel cell and optimal strategies. The A-ECMS provided good results although they were lower than the constant fuel cell strategy. The benefits of adaptive estimation are not significant enough to warrant the additional

complexity required for estimation when compared to the simpler battery load following strategy.

Hydrogen fuel cell vehicles have the real potential to become the next major vehicle technology. Only by continuing to research every aspect of these vehicles needed to make them viable for consumer use can these vehicles ever replace the gasoline powered vehicles we use today.

Acknowledgements

I would like to acknowledge the hard work of all the members of the University of Waterloo Alternative Fuels Team throughout the EcoCAR competition. Each member of the team worked very hard, dedicating countless hours towards building the fuel cell powered vehicle which eventually won third place in the competition. Without their work, none of my research would have been possible. I would especially like to thank Michael Giannikouris, Alex Koch and Gurhari Singh who's direct support beyond the scope of the competition helped me complete my research.

I would also like to thank the competition sponsors for their constant support of the team and CrossChasm Technologies for sponsoring my research and training me in the tools I needed to use to develop the control strategies evaluated as part of my research.

Finally I would like to thank my supervisors Dr. Steven Waslander and Dr. Roydon Fraser for providing me with the opportunity to be a part of the EcoCAR competition and work on this amazing project for my master's research.

Dedication

I would like to dedicate this thesis to my parents, Joanna Karpinska and Raymond Leydier. Finishing this thesis and my master's degree would not have been possible without the constant support that they have given me. I truly appreciate everything they have every done and every sacrifice they have ever made to help me get as far as I have. Thank you.

Table of Contents

List of Tables

List of Figures

Chapter 1

Introduction

The way modern society looks at transportation is changing. Gasoline prices are constantly increasing as the availability of fossil fuels becomes more of a concern. Concerns over global climate change, the impact on people's health and other environmental effects caused by burning fossil fuels are forcing the automotive industry to make a dramatic shift in the way vehicles work at a fundamental level. To combat these various issues the automotive industry is putting an ever increasing emphasis on the development of alternative fuel technologies.

1.1 Why Hybrids are Important

Conventional internal combustion vehicles burn fossil fuels which produce emissions that have a serious impact on the environment and people's health [12]. Hybrid vehicles are the automotive industry's short term solution to these issues [33]. Hybrid vehicles allow us to reduce our energy footprint by providing an extra energy source in addition to the internal combustion engine. The goal of a hybrid vehicle is to use a battery system to store energy that would otherwise be wasted which reduces society's impact on the environment by reducing overall fuel consumption and the resulting tailpipe emissions. One way in which this is accomplished is by using a technique called regenerative braking which recaptures a portion of the propulsion energy when braking. With plug-in hybrids, it is even possible to use electricity taken directly from the electrical grid to charge the battery, further reducing fossil fuel use. Substantial work is being done to make plug-in hybrid vehicles viable for large scale use [9]. By using the added battery system, hybrid vehicles can reduce fuel consumption and emissions in order to provide for a cleaner, more environmentally friendly and energy efficient vehicle.

1.2 The Benefits and Limitations of Hydrogen

While hybrid vehicles are still being deployed by automotive manufactures to address fuel consumption and emission concerns, these vehicles still produce harmful emissions and use fossil fuels. Without a better solution, oil reserves will still eventually be depleted and the use of both hybrid and non-hybrid vehicles will continue to have a negative impact on the environment.

To completely eliminate harmful vehicle emissions and dependence on gasoline a new clean fuel source is needed. One such possible fuel source is hydrogen. Studies have determined that hydrogen is the only current fuel source capable of substantially reducing global GHGs and urban air pollution [8, 37, 52]. Hydrogen fuel cell vehicles do not have any harmful tailpipe emissions and only produce water vapor at the exhaust. Since fuel cell vehicles run entirely on electricity either stored in their high power battery or produced directly from hydrogen, they are completely free of dependence on gasoline. This makes hydrogen a very promising fuel source for future hybrid vehicles [54].

Hydrogen still has some limitations that prevent it from replacing gasoline as the current main automotive fuel. The main limitation of using hydrogen is that there are very few places where hydrogen fuel cell vehicles can be fueled. To develop the proper infrastructure to fuel hydrogen fuel cell vehicles a significant financial investment is required. While this financial investment is not substantial compared to the cost of maintaining existing fuel stations, the initial investment is still a barrier to the global adoption of hydrogen as the main vehicle fuel [37, 52]. As hydrogen vehicles become more viable, gas stations in areas where these vehicles are used are slowly starting supporting hydrogen and this is expected to continue as long as hydrogen fuel cell vehicles continue to be produced. Hydrogen, when not stored properly can also be a very dangerous fuel source and there is still some concern over the safety of using hydrogen in vehicles. Automotive manufacturers are doing substantial work to achieve the high level of safety required in hydrogen storage systems for hydrogen fuel cell vehicles and currently have plans to deploy fuel cell powered vehicles to the public as early as 2015 [38]. Hydrogen fuel cells are also currently very expensive to manufacture and additional work is still needed to bring the cost of fuels cells down to a more reasonable level. Once the limitations preventing hydrogen from replacing gasoline are overcome, hydrogen could become the solution to the issues that currently plague the automotive industry.

1.3 Hybrid Vehicle Control

One critical aspect of developing hybrid vehicles is the hybrid vehicle control strategy. All hybrids have multiple energy sources which they use to reduce their primary fuel usage. The extra energy source is typically a large battery which can be treated not only as a source but also as a means of temporarily storing energy. The ability to temporarily store energy allows for the vehicle to take advantage of operating the primary energy source at higher efficiency points where the excess energy can be stored and later used. At the same time, this allows for the implementation of regenerative braking where energy initially used to propel the vehicle can be recaptured when braking and reused [12]. While these technologies allow for significant improvements in fuel economy, this is only true if they are used correctly [12]. To realize the benefits of having the extra degrees of freedom the hybrid architecture provides, the control software of the vehicle must intelligently decide how to satisfy the power demand requested by the driver [12]. To realize the full potential of hybrid vehicles it is necessary to develop effective control strategies that take full advantage of the capabilities of both power sources. Automotive manufacturers and researchers around the world are currently working on developing strategies to achieve the peak efficiency possible for many different types of hybrid vehicles.

1.3.1 Conventional Hybrid Control

Control strategies for traditional series and parallel hybrid vehicles with internal combustion engines have been studied extensively [31, 44]. Most current hybrid vehicles use control strategies that are rule-based since these are simple to implement and test [16]. While rule-based strategies produce effective results in reducing fuel consumption compared to non-hybrids, they are limited in what they can achieve compared to some of the more complex strategies. Rule-based strategies typically only consider the current operating mode, current power demands and battery state of charge when making decisions on how to operate the vehicle. They do not include future power demands in their decision making process since this information is not readily available. These strategies also do not typically consider the long term durability of the battery. The majority of hybrid control research has been primarily focused on optimization of simulations to determine the peak performance of different hybrid architectures. One example of this is the convex optimization method for determining peak powertrain performance proposed by Tate and Boyd [51]. Another is the different implementations of Dynamic Programming that have been developed to analyze hybrid vehicle performance [40, 16]. Particle swarm optimization has also been used for this purpose [55, 21]. Other methods based on optimal control theory have also been studied [45]. These methods are only meant for simulations and cannot be used for real world operation since they depend on complete knowledge of the drive cycle and an extensive amount of computation. Several strategies that are designed to be run in real time have also been studied. One promising strategy is the equivalent consumption minimization strategy (ECMS) [48, 4]. Others include modified versions of ECMS including the Adaptive Equivalent Consumption Minimization Strategy (A-ECMS) and the Telemetry Equivalent Consumption Minimization Strategy (T-ECMS) [11, 19]. The ECMS and its variants attempt to find a compromise between the optimal and rule-based strategies by converting battery power usage to an equivalent fuel usage and optimizing over the instantaneous power demand. These strategies demonstrate near optimal fuel consumption for standard drive cycles and have been tested on a prototype Mercedes A-Class vehicle and a prototype pre-transmission hybrid based on 2002 Ford Explorer. This research has primarily focused on vehicles with conventional internal combustion engines and very few of these strategies have been evaluated against other types of vehicle architectures.

1.3.2 Hydrogen Fuel Cell Hybrid Control

Due to the relatively recent development of fuel cell packs sufficiently light and efficient enough to power passenger vehicles, there is little prior work on control strategies for hybrid fuel cell vehicles. Lin et al. presented a stochastic approach to fuel cell hybrid vehicle control based on Markov chain modeling and stochastic dynamic programming [10]. The results presented showed improvements over rule-based controllers but were only presented in simulation. Hong-wen et al. presented a control method for a small fuel cell powered bus [22]. Two rule-based strategies were used, but no comparison to optimization based solutions was presented. Mallouh et al. studied the effect of control strategies on the performance of a fuel cell powered auto rickshaw. Several strategies were evaluated including a variation of the ECMS and several simple strategies [32]. Mallouh et al. demonstrated that for his particular vehicle architecture a simple strategy can provide better fuel economy numbers than more complex optimized strategies such as ECMS [32]. For the auto rickshaw, a strategy where the fuel cell follows the trace of the power demand was shown to provide the best fuel economy. While it is expected that similar efficiency results will be seen for conventional SUVs, differences in the architecture, driving patterns, mass and road loads as well as the fuel cell architecture itself are expected to result in some differences as to which particular control strategies are shown to be most efficient.

1.4 Overview

Three control strategies are presented here in this thesis for use on hydrogen fuel cell powered vehicles. The first strategy is a mode switching rule-based strategy that switches between charging and discharging the battery based on the battery state of charge. The second strategy is a constant fuel cell power output strategy that runs the fuel cell at the average power demand for the drive cycle and uses the battery to manage transients in the power demand. The third and final control strategy is an adaptive equivalent consumption minimization strategy originally demonstrated by Musardo et al. and has been modified in this thesis to run on fuel cell based vehicles [11]. These strategies are implemented in simulation in Matlab and then evaluated against optimized simulations developed using quadratic programming optimization methods. It was discovered that operating the fuel cell at a near peak efficiency using the constant fuel cell strategy provided the best fuel economy results. The results of the far more complicated adaptive equivalent consumption minimization strategy, while good, were consistently below the constant fuel cell strategy results.

The constant fuel cell strategy and mode switching rule-based strategy have also been implemented in real-world experimentation on a modified 2009 Saturn Vue which has been refit with a completely new fuel cell based plug-in hybrid powertrain. The modified 2009 Saturn Vue is a fully functional Li-Ion/Fuel Cell Hybrid SUV developed by the University of Waterloo Alternative Fuels Team. A significant amount of work has been done by the team to build this vehicle which can be seen in Figure 1.1. The fuel cell hybrid vehicle contains a 250 V lithium ion battery pack, an OEM designed hydrogen fuel cell stack with an electric traction system for a front axle motor, a Brusa DC/DC converter and a Ballard electric motor paired with a Rinehart inverter for a rear axle motor. Control strategy testing was done on-road using a custom drive cycle. The experimental results showed remarkably similar results to the simulations, demonstrating that the constant fuel cell strategy is an effective strategy.

The research presented in this thesis has found that simpler, more practical strategies produce very effective results for hybrid hydrogen fuel cell vehicles. More complex strategies still produce good results however the added requirements for additional sensing methods and more complex testing procedures that can ultimately reduce reliability make these strategies impractical. The effectiveness of these simple strategies has been demonstrated both in simulation and with experimental results produced using the hydrogen fuel cell powered vehicle developed by the University of Waterloo Alternative Fuels Team.

Figure 1.1: Modified 2009 Saturn Vue Fuel Cell Test Vehicle[53]

Chapter 2

Background

2.1 History of Hybrid Vehicles

Hybrid vehicles have been around since the 1898 with the first hybrid being built by Dr. Ferdinand Porsche. This hybrid car was the second car Dr. Porsche ever built and contained an internal combustion engine powering a generator which worked in tandem with a battery to power small electric traction motors located in the wheel hubs [1]. At the time, the electric motor/generator in the vehicle was a key component of starting the vehicle's internal combustion engine. This all changed in 1913 when self-starting gasoline powered vehicles were introduced. These simple and cheap vehicles became much more popular than the hybrid, steam and electric vehicles of the time [1]. It wasn't long before the only people working with hybrid vehicles were researchers and hobbyists [1]. It wasn't until the 1973 oil embargo when rapid increases in oil prices rekindled global interest in alternative energy vehicles and by extension hybrid vehicles. This was followed by governments passing numerous resolutions and laws as well as creating incentives for cleaner more energy efficient vehicles [1]. In 1997 Toyota introduced the very successful Prius hybrid electric vehicle to the consumer automotive market. Since then several hybrid vehicles using different technologies have been developed and made available to the general public [1].

2.2 Different Types of Hybrid Vehicles

The term hybrid vehicle refers to any vehicle that uses two or more power sources to provide propulsion power to the vehicle. This includes all types of batteries and internal combustion engines, fuel cells, solar panels, compressed gas based energy storage systems such as compressed air and any other energy source which can be mounted to a vehicle to provide propulsion power. While hybrid vehicles can use a variety of energy sources, all hybrid vehicles can be categorized as either a series hybrid or parallel hybrid vehicle. The terms series and parallel refer to the number of unique energy paths used to provide propulsion. Hybrid vehicles can further be classified depending on whether or not they have battery systems that can be charged from the electric grid using either an on-board or external charger. Hybrids that have this capability are called plug-in hybrids. One example of this type of vehicle is the Chevrolet Volt.

2.2.1 Series Hybrids

A series hybrid vehicle uses a single energy path to the wheels. This means that while the vehicle has multiple energy sources such as a battery and an internal combustion engine, only one path can exist for the wheels to receive the energy provided by those sources [30]. At some point before the wheels, the energy paths must merge to form a single path. For example, in a conventional series hybrid electric vehicle, the mechanical energy from the internal combustion engine is converted to electrical energy through a generator. This electrical energy charges the battery which directly powers the wheels through an electric motor. An example of a series powertrain architecture can be found in Figure 2.1.

2.2.2 Parallel Hybrids

Parallel hybrid vehicles are those vehicles which have multiple parallel energy paths to the wheels. A conventional parallel hybrid vehicle will have both a battery that can power a motor which can drive the wheels and a direct mechanical linkage to the wheels from the engine. The two paths are typically connected through a torque coupling system which then leads to the wheels. In this way there are two distinct energy paths available for propulsion.

An example of a parallel hybrid architecture can be found in Figure 2.2. There are many different types of parallel vehicles which can each be classified by the way in which they achieve their parallel operation.

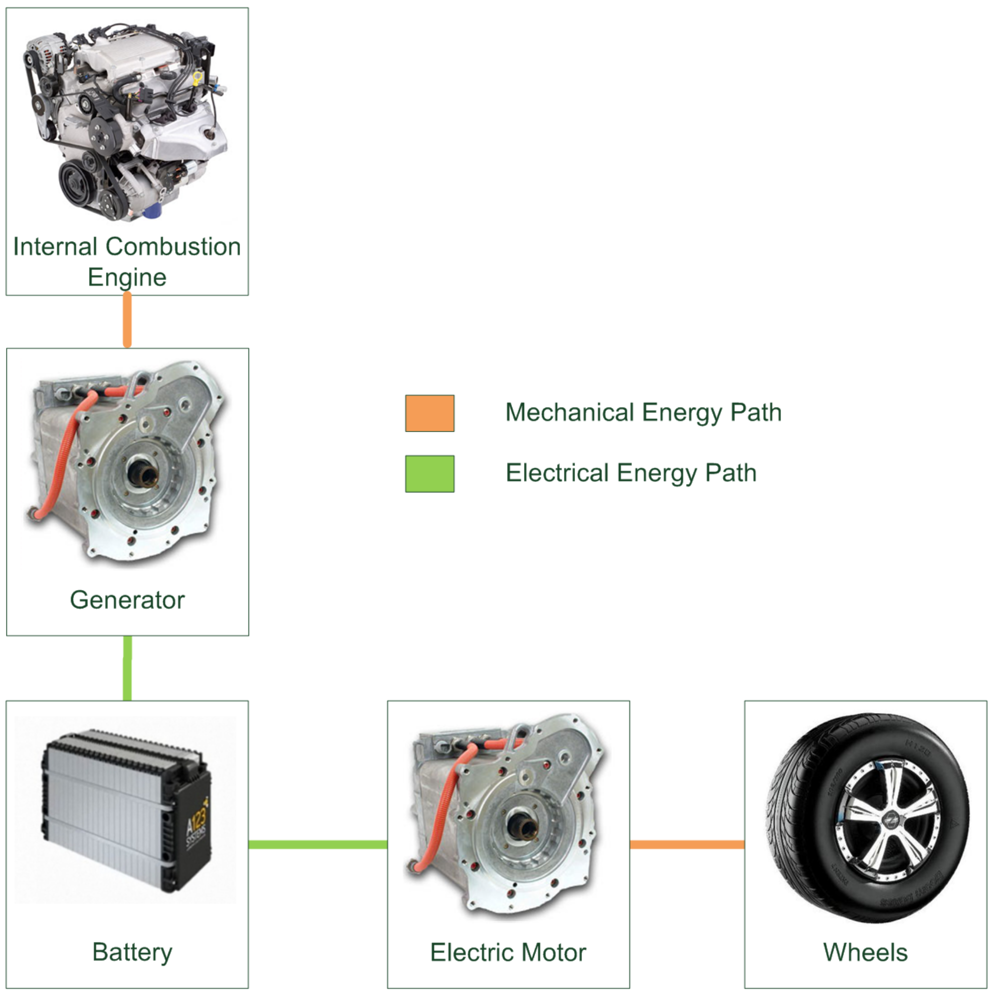

Figure 2.1: Example of a Series Powertrain

Pre-transmission parallel architectures like the one shown in Figure 2.2 place the transmission between the torque coupler and the wheels. Post-transmission parallel architectures instead place the transmission between the engine and the and the torque coupler. The post-transmission architecture provides more control over the engine operating point but is only viable for more heavily hybridized vehicles with larger electric motors which can provide a substantial amount of torque [30]. Pre-transmission architectures on the other hand are better suited for hybrids with small motors which only act to start and assist the engine while also taking advantage of regenerative braking. These vehicles are often referred to as mild hybrids [30].

Another type of parallel architecture is the separated axle parallel hybrid architecture, shown in Figure 2.3. These vehicles have two distinctly separate powertrains. The rear half of the vehicle is typically powered electrically by a battery and motor. The front half is powered mechanically by the internal combustion engine. Energy can be transferred to the battery through regenerative braking [30].

One of the more popular parallel architectures is the power-split or series-parallel architecture. This architecture combines the standard parallel architecture and the series architecture to get the benefits of both systems. This is the architecture used by the Toyota Prius hybrid vehicle [34]. Figure 2.4 demonstrates the layout of this architecture. While this architecture is more complicated than the others it allows for both directly charging of the battery using the generator and directly driving the wheels using the engine. The benefit of this is that it minimizes efficiency losses and allows the vehicle to operate as either a full series of a full parallel depending on what will provide the best fuel economy and lowest emissions at any given time [34].

2.2.3 Hydrogen Fuel Cell Hybrids

Hydrogen fuel cell hybrid vehicles are a unique version of the series architecture. The primary difference between fuel cells and internal combustion engines from a powertrain design perspective is that while internal combustion engines produce mechanical energy which must later be converted to electrical energy to charge the battery, fuel cells directly produce electrical energy. This fundamental difference eliminates the need for a generator to charge the battery from the fuel cell. The generator is instead replaced with a DC/DC converter to regulate the voltage between the fuel cell and battery. A simple fuel cell architecture is shown in Figure 2.5.

The fact that both devices use electrical energy inherently means that hydrogen fuel cell hybrid vehicles are mostly built as series vehicles with only one electrical energy path.

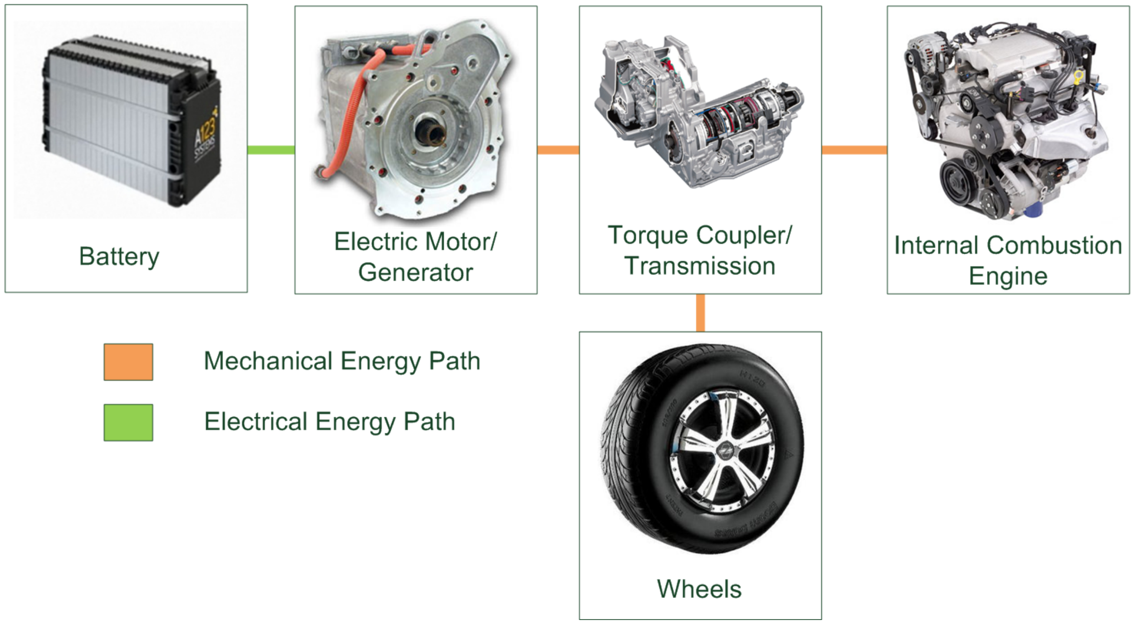

Figure 2.2: Example of a Parallel Powertrain

Removing the conversion from mechanical to electrical energy between the fuel cell and battery inherently results in fewer losses when charging the battery in this architecture.

Besides the fewer efficiency losses through energy conversion, fuel cell hybrids have several other benefits over conventional hybrids [29]. Fuel cells do not have as many moving parts which not only reduces noise and vibrations but also the need for maintenance as there is less wear on the internal components. Hydrogen fuel cells also do not have the harmful emissions that internal combustion engines produce. The only tailpipe emission produced by a hydrogen fuel cell vehicle is water vapour.

Hydrogen, however, does still have some disadvantages that must be overcome before it can become a practical fuel source. The main disadvantage of using hydrogen as a fuel source is that the infrastructure required to fuel hydrogen vehicles does not yet exist. There is a substantial financial investment required to upgrade the existing gas stations to support hydrogen fueling. In addition to this, there is still some public concern over the safety of using hydrogen as a fuel source. A very high level of safety is required in the hydrogen storage system to protect against hydrogen leaks and damage to the compressed hydrogen storage tanks.

While there are still some disadvantages in using hydrogen as a fuel source, with ad-

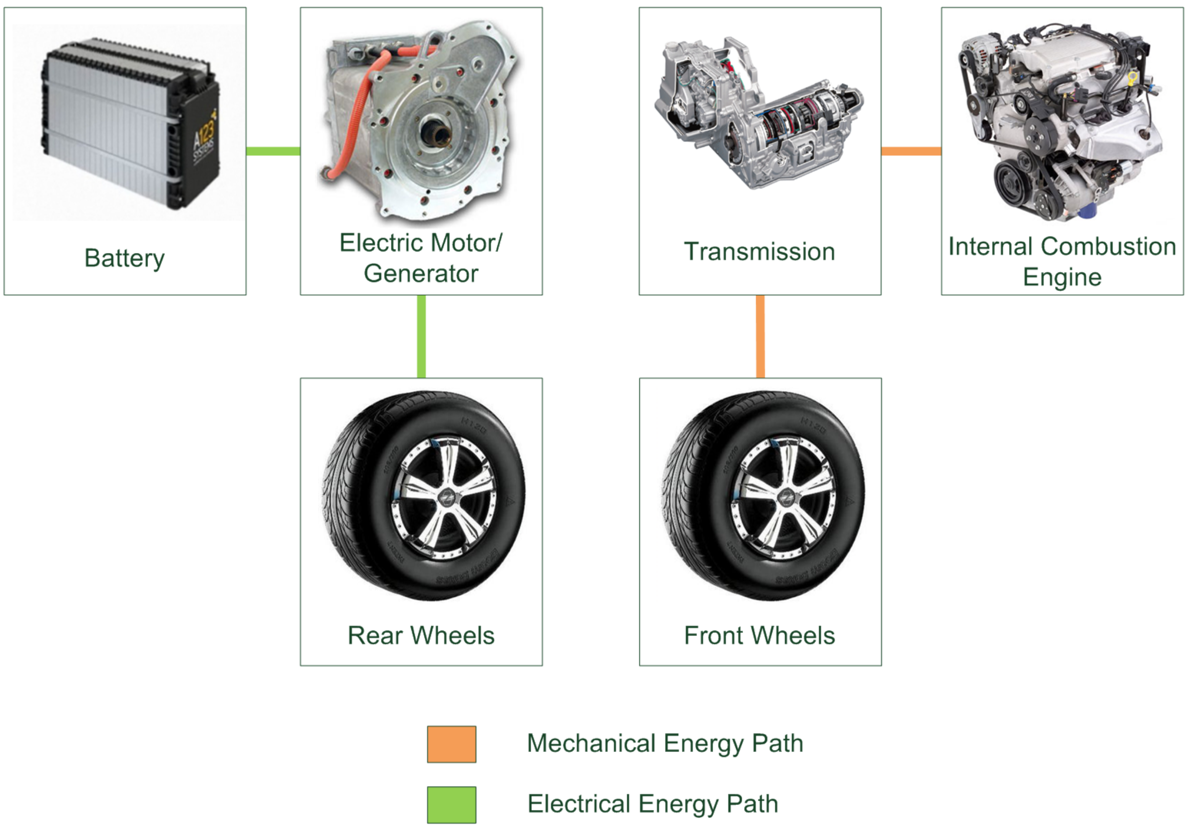

Figure 2.3: Example of a Separated Axle Parallel Powertrain

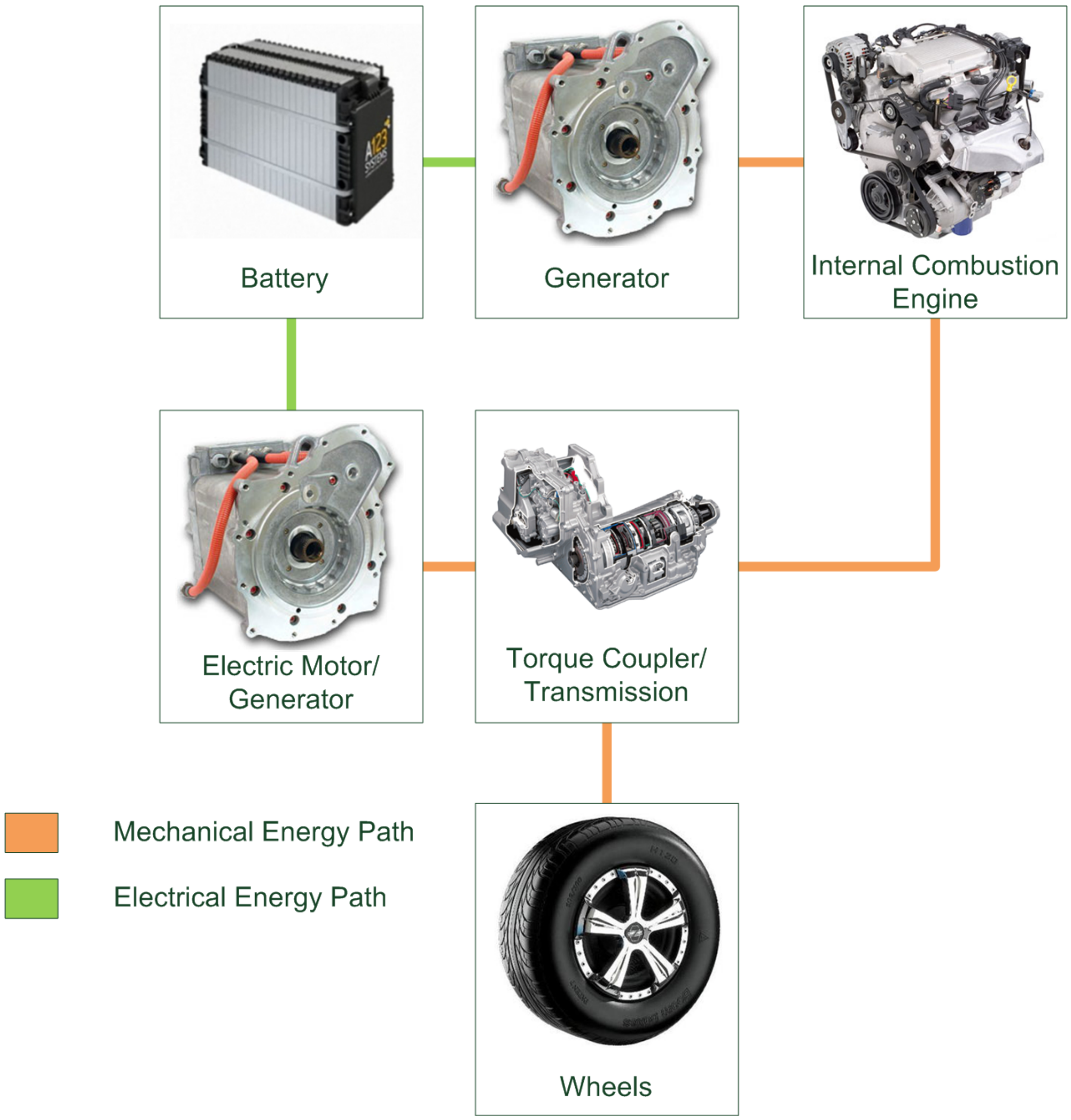

Figure 2.4: Example of a Power-Split or Series-Parallel Powertrain

ditional research, the benefits of hydrogen fuel cells can make hydrogen a very promising future power source for hybrid vehicles.

2.3 Conventional Hybrid Control Strategies

With the automotive industry pouring substantial funding into hybrid vehicle development, a significant amount of research has been done in all aspects of hybrid vehicle development, including battery modeling and sizing of battery systems for expected vehicle drive cycle loads [2, 36]. Significant work has also been done on battery state of charge and capacity estimation [46, 35]. One field that has received a significant amount of attention is powertrain control.

The seemingly simple change of adding a battery to act as a secondary power source introduces a new degree of freedom for vehicle control. It is now possible to decouple the engine's operating point from the instantaneous power demand and use the battery's power storage capabilities to operate the engine at far more efficient operating points as well as recapture propulsion energy through regenerative braking. The problem of how to make the most of this new degree of freedom by getting the best fuel economies and the lowest emissions without sacrificing performance and reliability is a very difficult problem to find a good solution for. Finding the best solution to this hybrid control problem is an important area in automotive controls research.

2.3.1 Rule-Based Control

Most modern hybrid vehicles employ rule-based control strategies which trigger based on battery state of charge (SOC) changes and component power limits. One typical control strategy used by hybrid vehicles is the on/off strategy which is found on the Toyota Prius [39]. This basic strategy turns on the engine only when the vehicle's battery is at a low state of charge or the power demand of the vehicle cannot be satisfied by the battery alone [12]. The engine is operated at a high efficiency point and turned off when it is no longer needed. Another strategy that is typically used on hybrids is the blended or continuous operation strategy which runs the engine at all times, except possibly when idling, and uses the battery to supplement power demands to better control the operating point of the engine as well as to take advantage of regenerative braking. The strategy selected depends in part on the exact nature of the hybrid vehicle's architecture.

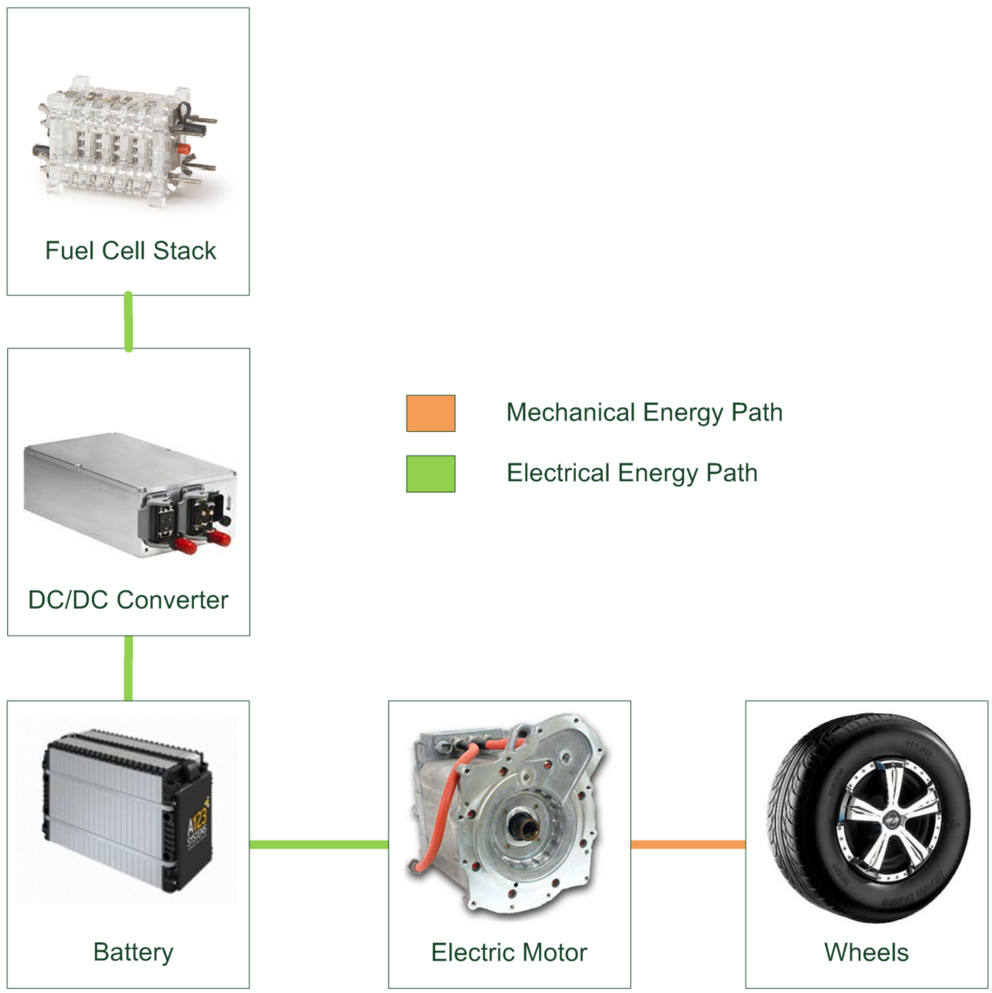

Figure 2.5: Example of a Fuel Cell Powertrain

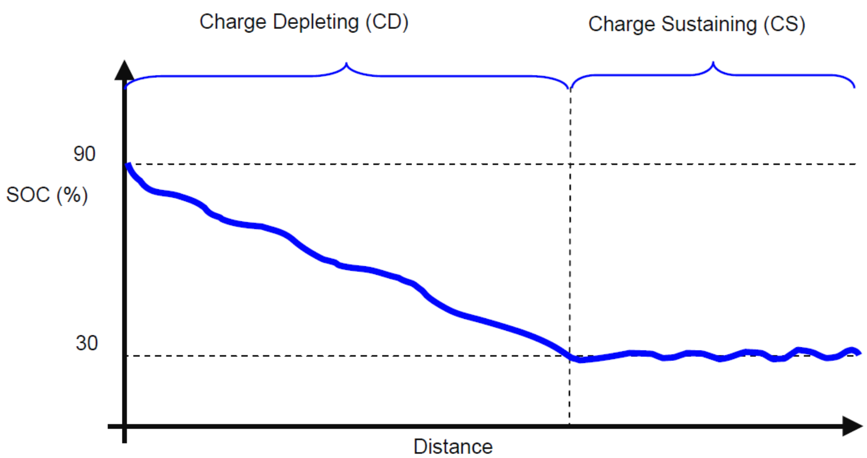

Figure 2.6: Example of Plug-in Hybrid Vehicle Operation Modes [3]

A special note needs to be made about control strategies for plug-in hybrid electric vehicles (PHEVs). For the most part plug-in hybrid control strategies function the same way as other hybrid control strategies [3]. The main difference in PHEVs is that PHEVs can be charged via an external charger and as such can initially have additional energy stored in the battery. PHEVs typically have much larger battery systems as a result and can travel a notable distance entirely on battery power. During the early stages of a driving mission, the vehicle typically operates in a charge depleting mode where, either through blending or operating in an electric only mode, the vehicle discharges the battery from its higher charge level to a lower level. Once at the lower charge level the vehicle switches to a more conventional hybrid control strategy. This second mode is referred to as the charge sustaining mode. A plot of the battery state of charge for an example of this type of operation is shown in Figure 2.6.

2.3.2 Optimal Control

A significant amount of research has been done on vehicle control in recent years. This is in no small part due to rising energy prices and the resultant reintroduction of hybrid vehicles into the normal consumer market. Much of this research has revolved around using optimization techniques to improve vehicle fuel economy.

	Fuel Economy	Units
Hybrid Optimal Solution	44.44	mpg
Non-Hybrid Vehicle	41.55	

Table 2.1: Convex Optimization Results for Partial FTP Drive Cycle [51]

Convex Optimization

The most direct method of finding the optimal solution to the hybrid control problem is to directly use a nonlinear convex optimization technique. This method was demonstrated by Tate and Boyd where they use this approach to find the optimal fuel consumption of a series hybrid powertrain [51]. Tate and Boyd begin by first defining their system model as their key powertrain components; a spark ignition engine, a lead acid battery and an electric motor. The key operating constraints of these components are then defined. This includes battery storage and charge/discharge rate limits, engine power and slew rate limits as well as regenerative brake power limits. A drive cycle is then expressed in terms of power demands from the battery, engine and motor and a continuous time cost function is defined as the total fuel consumption of the engine throughout the drive cycle. This forms the basis of the optimization problem. The goal of the optimizer is to solve the optimization problem so as to minimize the fuel consumption while satisfying the constraints of the system [51]. While this problem is solvable, it is still complex. To simplify this problem for use with common optimization tools, Tate and Boyd redefine the problem as a Linear Program by discretizing it and redefining the constraints in LP form [51]. To demonstrate the validity of this approach Tate and Boyd performed an optimization for their vehicle using the first 1371 seconds of the FTP drive cycle [51]. Table 2.1 shows the results of Tate and Boyd's optimizer compared to the same vehicle in a non-hybrid configuration. In their conclusions it is noted that the problem definition did not allow for turning off the engine which explains the low fuel economy produced by the optimizer. Tate and Boyd claim that with additional this approach can be expanded to include on/off operation which will allow for much better fuel economy results [51].

Dynamic Programming

One of the most common optimization techniques used in vehicle controls research is dynamic programming. Dynamic programming is a class of optimization methods that work by breaking the optimization problem down to several smaller problems that can be solved or optimized sequentially [40].

Control Strategy	UDDS	US06	ECE-EUDC	HWFET	Average	Units
Dynamic Programming	4.27	4.47	3.76	2.88	3.845	L/100km
Rule-Based Strategy	4.3	10.5	7.8	7.9	7.625	
Conventional SUV	11.7	12.8	11.9	8.6	11.25	

Table 2.2: Dynamic Programming Simulation Results [40]

These approaches work by constructing a cost function based on the instantaneous fuel consumption for the driving mission. The cost function is defined as a summation of the current cost and a cost to go to the end point. The optimization starts from the end point and works backward to all possible solutions reachable in the previous time step. It relies on the principle of optimality, which states that the final solution to the optimization problem can only be optimal if all the solutions to the separate sub-problems in the full optimization problem are optimal.

Dynamic programming's main flaw is that it is computationally intensive [11]. Qiuming Gong uses dynamic programming in his paper entitled Optimal Power Management of Plug-in HEV with Intelligent Transportation System where he proposes an improved control strategy based on dynamic programming which uses traffic and GPS data to predict road loads [40]. His strategy was implemented on a model of a parallel plug-in hybrid SUV and tested against the UDDS, US06, ECE-EUDC and HWFET drive cycles. Table 2.2 shows the results of Gong's research.

Based on his results the average fuel economy of the dynamic programming based control in the charge depleting mode is 3.845 L/100 km which corresponds to a 49.6% improvement over a typical rule-based control strategy and a 65.8% improvement over a typical SUV [40]. These results demonstrate that there is a considerable improvement in fuel economy of hybrids over non-hybrid vehicles. At the same time, as effective as basic rule-based strategies are, there is still room for improvement and advanced optimization based strategies such as the one proposed by Qiuming Gong demonstrate this. This however comes at a cost of complexity since Gong's strategy carries with it the requirement for accurate, up to date, and consistently available GPS and traffic data or another alternative means of predicting the drive cycle to a highly accurate degree [40]. Despite this, Gong does still demonstrate the limitations of simple rule-based strategies and that better strategies are needed to achieve the best possible results.

Dynamic programming was also implemented by Dominik Karbowski from Argonne National Labs and optimizes based on changes in the state of charge for the battery [16]. Using dynamic programming, Dominik Karbowski finds the optimal solutions for use on a plug-in parallel pre-transmission hybrid for various standardized drive cycles. This optimal solution is then evaluated and used to create an improved rule-based strategy which Karbowski uses in the PSAT simulation tool [16]. The intent is that these drive cycles for which the simple strategy has been optimized will closely reflect the driving patterns of the actual drivers of the vehicle. This in turn yields a better fuel economy and lower energy consumption. Figure 2.7 shows the power consumption for the total vehicle, the engine and the battery in both the optimal solution and the simulated rule-based strategy. The results are shown on a plot against the distance traveled for ten consecutive NEDC drive cycles.

Karbowski developed his optimized rule-based strategy for a range of close to 40 km [16]. Karbowski's results show that his simulated rule-based strategy shows very promising results up to about 40 km at which point the vehicle switches from a charge depleting mode to a charge sustaining mode and starts consuming substantially more energy from the engine. The optimal solution instead uses the battery power much more gradually and does not need to switch into the charge sustaining mode of operation. The optimal solution is able to retain better control over the engine operating points throughout the remainder of the driving mission as shown in Figure 2.8. The end result is that the rule-based strategy consumes substantially more overall energy than the optimal solution.

Based on these results, the inability to predict the mission length leads to a strategy that operates the engine at some highly inefficient points towards the end of the mission which resulted in a 60% increase in input energy consumption [16]. Karbowski states in his conclusions that it is best to gradually discharge the battery to its lowest acceptable state of charge throughout the entire driving mission [16]. It is therefore best to always operate in a charge depleting mode since this provides the best flexibility for controlling the engine's operating point, while still using the energy stored in the battery as much as possible. Since the mission length is not known, it is difficult to develop a simple optimal solution for all operating distances. Karbowski's results demonstrate that simple SOC and power limit rule-based strategies are inherently flawed and there is significant room for improvement.

Particle Swarm Optimization

Another optimization method that has been proposed is a modified version of particle swarm optimization [55]. The principle logic behind particle swarm optimization is that a set of solutions for the power split problem are created with a position and velocity in a multidimensional solution space. Each solution is evaluated based on fuel consumption and each solution is updated based on the velocity and distance from the current best

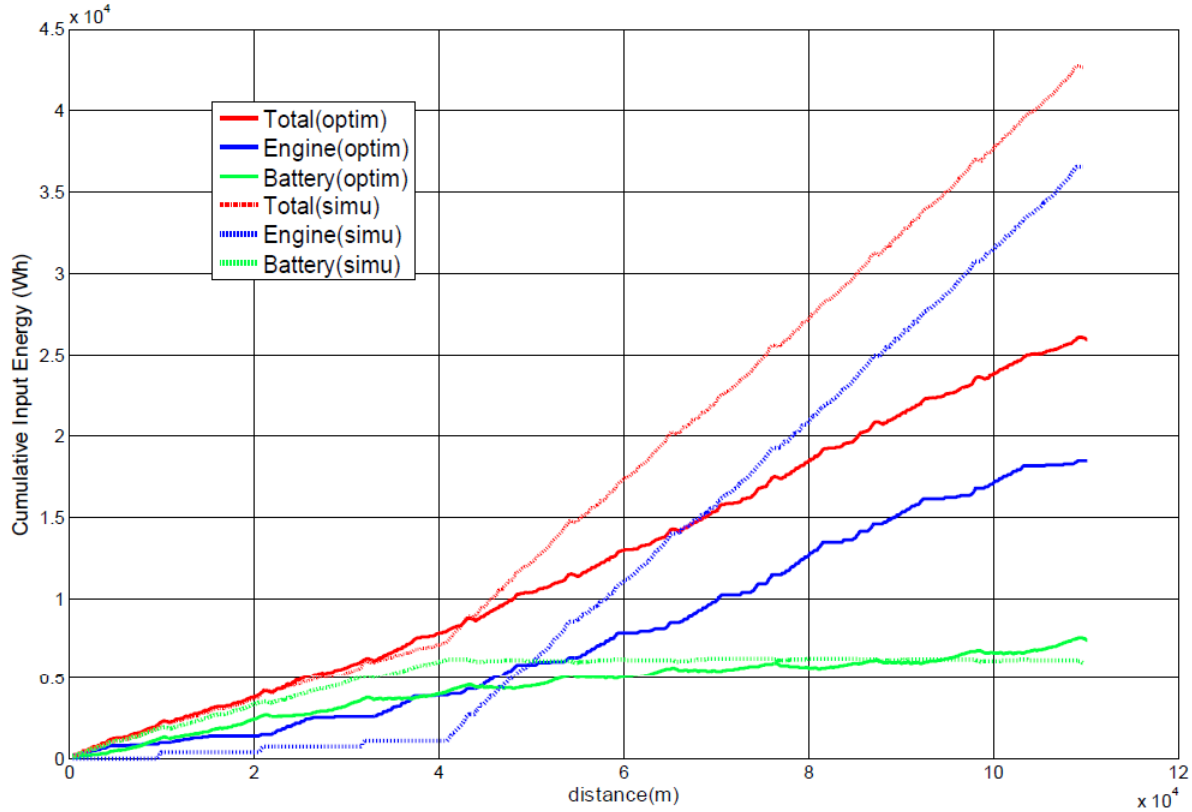

Figure 2.7: Input Energy Consumed for Rule-Based Simulation and Optimal Solution [16]

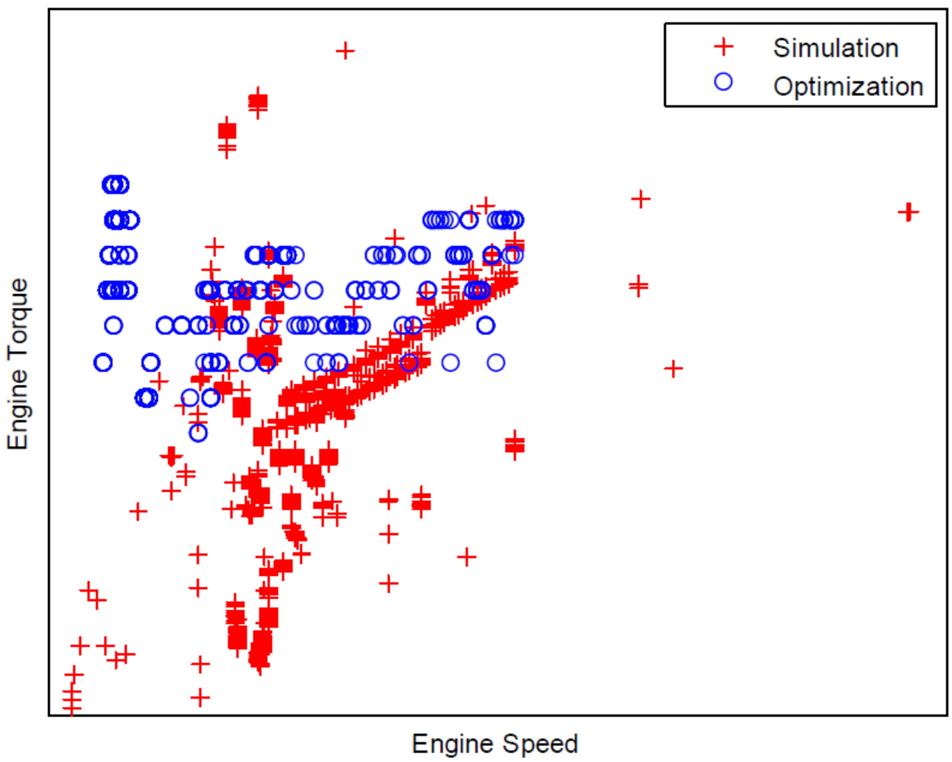

Figure 2.8: Engine Operating Points for Rule-Based Simulation and Optimal Solution [16]

	PSAT Controller	Particle Swarm	Units
Fuel Consumption	160.7	192.8	mpg
Electrical Consumption	114.64	119.10	Wh/mile
Powertrain Path Efficiency	49.53	53.72	%
Energy Recovered at Battery	34.29	61.92	%

Table 2.3: Simulation Results for Particle Swarm Optimization [21]

solution. This is repeated for several iterations until the optimal solution is found within a defined degree of certainty [55]. In 2009, Banvait et al. demonstrated this approach for a parallel plug-in hybrid and compared the results against the rule-based control strategy used by the PSAT vehicle modeling and simulation tool [21]. The vehicle model was run with both strategies against a UDDS drive cycle. The results are shown in the Table 2.3.

Banvait et al. demonstrates that the particle swarm optimization yields a significant gain of 32.8 mpg which corresponds to a 4.19 % increase in bidirectional path efficiency and a 27.63 % increase in energy recovered by the battery [21]. This demonstrates that there is substantial room for advancement over basic rule-based control strategies particularly for plug-in hybrids.

Limitations of Optimal Control

The implementations of convex optimization, dynamic programming and particle swarm optimization all show that there is notable room for improvement over standard rule-based strategies for conventional hybrid vehicles. In many cases the rule-based strategies only performed well for specific drive cycles, examples of which can be seen in Table 2.2 and Figure 2.7.

As effective as optimal control techniques are, they have one significant limitation that is common among all the techniques that have been discussed. This limitation is that in order to determine the optimal solution it is necessary to have complete knowledge of the drive cycle. While it is possible to obtain the required knowledge to perform these optimizations in real-time, the complexity of the sensing systems needed to predict the drive cycle with the required accuracy makes real-time implementation impractical. As such, these optimization methods are only usable as benchmarking tools and guidelines that can be used to develop and evaluate other control strategies. To overcome these limitations more advanced strategies that can be run in real-time have been developed.

Driving Cycle	Dynamic Programming	ECMS
UDDS	1	1.017
US06	1	1.017
FTP highway	1	1.009

Table 2.4: Relative Comparison of Dynamic Programming and ECMS Fuel Consumption [28]

2.3.3 Equivalent Consumption Minimization Strategy

One strategy that was proposed to overcome many of the downfalls of other optimal strategies is the equivalent consumption minimization strategy (ECMS). This strategy was demonstrated by Antonio Sciarretta [48]. The basic premise of this strategy is that energy stored in the battery comes at the cost of fuel consumed at another point in the vehicle's operation [48]. Using this knowledge, the global optimization for the power split over the entire driving mission can be reduced to a series of instantaneous optimizations where battery usage is given an equivalent fuel cost. The battery energy is added to the fuel consumption optimization calculation as shown in Equation (2.1).

$$E_{Total} = E_{ICE} + s \times E_B \tag{2.1}$$

This equation shows the change in total instantaneous fuel energy used by the vehicle as a function of fuel energy consumed by the engine and equivalent fuel energy consumed by the battery. The s term is called the equivalence factor which is used to convert battery energy to equivalent fuel energy [48]. Each driving mission has two equivalence factors, one that is used when charging the battery and one that is used when discharging the battery. The value of the equivalence factors used to achieve optimal performance are dependent on the driving mission and can be determined by experimentation [48].

Serrao et al. performed a comparision between the ECMS and dynamic programming methods which is presented in Table 2.4 [28]. All the values presented in Table 2.4 are normalized with respect to the Dynamic Programming results. The results presented in Table 2.4 demonstrate that the ECMS is capable of achieving fuel economy values that are very close to the results generated by optimal controllers which cannot be used in real-time.

Variations to the ECMS strategy have been developed to calculate equivalence factors while driving the vehicle based on data that is available to the vehicle's controller.

Control Strategy	FUDS	FHDS	ECE	EUDC	NEDC	JP10-15	Units
Dynamic Programming	25.7	26.0	24.5	24.8	24.5	25.2	mpg
ECMS	25.7	25.8	24.5	24.7	24.5	25.1	
A-ECMS	25.5	25.8	24.5	24.7	24.4	24.8	

Table 2.5: A-ECMS Simulation Results [11]

Adaptive Equivalent Consumption Minimization Strategy

One modified version of the ECMS strategy is called the Adaptive Equivalent Consumption Minimization Strategy (A-ECMS). This strategy is demonstrated in a paper by Musardo et al. and is implemented on a simulation of a pre-transmission parallel hybrid vehicle [11]. The basic principle behind A-ECMS is to simplify the ECMS optimization problem by adding an additional algorithm to generate a single equivalence factor in real time. The equivalence factor is determined by taking past and predicted data, along with the vehicle's current operating conditions and then using this to generate a prediction of the vehicle's mission while it is being driven. The algorithm presented requires GPS data and is designed to easily adapt to changes in the drive cycle [11]. Table 2.5 shows the results of the A-ECMS strategy for various drive cycles.

Based on the results presented in Table 2.5, the A-ECMS strategy shows a small decrease in performance when compared to the ECMS strategy, although it is still very close to the optimal result. In many cases the differences are not even measurable at the resolution presented in the report. This strategy is still limited by a requirement for GPS data which makes it difficult to implement.

Telemetry Equivalent Consumption Minimization Strategy

Telemetry ECMS (T-ECMS) is another variation on the ECMS strategy. This strategy is based on stochastic control methods [48]. The basic principle states that the equivalence factor can be simplified to a single value that is bounded between two values based on the optimal values that have been computed for similar driving conditions [4]. The idea is that these values are stored in the controller and selected based on patterns in the vehicle's operation. The equivalence factor can be calculated as a function of these two values and the probability that the battery is being discharged overall [4]. This is shown in Equations (2.2) and (2.3).

$$s = p \times s_{dis} + (1 - p) \times s_{chg} \tag{2.2}$$

Control Strategy	MVEG-A	ECE	JP10-15	Units
Optimal	3.18	2.82	2.90	L/100 km
T-ECMS	3.21	2.94	2.97	

Table 2.6: T-ECMS Simulation Results [4]

$$p = \frac{E_{max}}{E_{max} - E_{min}} \tag{2.3}$$

The optimal equivalence factors for the known similar drive cycle are represented by s_{chg} and s_{dis} for the charging and discharging values respectively while the probability that the battery is being discharged throughout the drive cycle is represented by p and the final resulting equivalence factor is represented by s. The maximum possible electrical energy used for the mission is represented by E_{max} while E_{min} is the minimum possible electrical energy used for the mission [4]. Simulated results for various drive cycles are show in Table 2.6.

Based on these results, T-ECMS provides a result that is very close to the optimal solution with the difference being close to 0.1 L/100 km. This strategy does still require some knowledge of the expected drive cycle and future road loads which makes it difficult to implement.

2.4 Fuel Cell Hybrid Control Strategies

Due to the relatively recent development of fuel cell systems designed for use in passenger vehicles, there is little prior work focusing on control strategies for hybrid fuel cell vehicles. Much of the fuel cell based hybrid vehicle research has focused either on the design of the vehicle itself or on the design or control of the inner components of the fuel cell. Many researchers have been involved in developing models of different fuel cell systems and researching long term performance degradation [18, 49, 26, 47]. Dumercy et al. in particular has done substantial research on thermal modeling of fuel cell systems. [27]. Other researchers have studied PEM fuel cell modeling from a control oriented approach [24]. Several reviews and comparisons of the different fuel cell models which have been developed, have been published [6, 13, 23]. Ahluwalia et al. has extensively studied the energy efficiency of fuel cell systems and how to best achieve peak efficiency operation by reducing parasitic loads and ensuring the fuel cell operates near its peak efficiency operating region as often as possible [42]. A substantial amount of fuel cell development research has focused particularly on the development, modeling and testing of various different membrane materials [43, 17, 5, 56]. Some researchers have performed extensive research on the design of fuel cell vehicles [7, 14, 15]. Sundstrom et al. in particular, has studied component sizing for fuel cell vehicles [50].

Despite the focus on lower level fuel cell design and control research, there are some researchers in the hybrid vehicle control field that have studied hybrid control for fuel cell based vehicles. The existing research includes simulations of theoretical control approaches based on optimal control theory as well as studies of rule-based strategies and their corresponding performance. There has, however been very little on-road testing done.

2.4.1 Stochastic and Rule-Based Control Strategies

Lin et al. presented a stochastic approach to fuel cell hybrid vehicle control based on Markov chain modeling and stochastic dynamic programming [10]. The approach taken by Lin et al. begins by developing a reduced-order fuel cell model for a theoretical fuel cell system including all the auxiliary components such as the compressor, humidifier and cooler. Models for a DC/DC converter, Li-ion battery pack, electric motor/inverter and the vehicle itself are then produced.

The driver's demand is modeled as a discrete-time stochastic dynamic process. The changes in the power demand are tracked in a Markov chain, which is a series of mathematical state equations that define a finite set of interconnected operating states [10]. The optimization process itself uses an infinite dynamic optimization problem where the cost function is a direct function of the hydrogen consumption rate and the deviation of the SOC from a desired reference SOC [10].

Lin et al. evaluates this approach against a simple rule-based control strategy defined by Equation (2.4) where $P_{FC,req}$ is the fuel cell power request, P_{mbr} is the electrical power demand of the motor, SOC_{des} is the desired SOC, $P_{FC,chg}$ is a constant power level and SOC_{min} and SOC_{max} represent the minimum and maximum limits of the SOC.

$$P_{FC,req} = \max\left(P_{mbr}, 0\right) + \frac{SOC - SOC_{des}}{SOC_{max} - SOC_{min}} \times P_{FC,chg} \tag{2.4}$$

The results of this work are shown in Table 2.7. The results presented showed improvements over rule-based controllers but made no mention of real-time implementations.

Drive Cycle	Rule-based (g/km)	Stochastic (g/km)	Improvement (%)
UDDS	9.33	8.86	5.0
LA92	12.64	12.14	4.0
HWFET	10.82	10.69	1.2
SC03	10.27	9.61	6.4
US06	18.79	18.09	3.7
NYCC	12.34	11.33	8.2

Table 2.7: Stochastic Simulation Results [4]

2.4.2 Fuel Cell Vehicle Modeling with Mode Based Control

Ning et al. developed a fuel cell vehicle model in Simulink and demonstrated its implementation using a simple mode based control strategy containing six unique operating modes [41]. The control strategy was developed to guarantee that at any given time the total power from the battery system and fuel cell would meet the traction motor power demand. The focus of the research was on developing an accurate model of the fuel cell and not evaluating the control strategy or fuel economy data.

2.4.3 Design and Control of a Fuel Cell Powered Bus

Hong-wen et al. designed a small fuel cell powered bus and proposed two rule-based strategies for controlling the bus's hybrid powertrain [22]. The first rule-based strategy operates the fuel cell between different modes with an On/Off operation and uses the fuel cell to follow changes in the power demand with the battery operating at a constant set-point proportional to its current SOC. This mode switching strategy is described by Figure 2.9. S_i is the on/off operating mode of the engine, k is the current time-step, P_f is the power demand and c_{SOC} is the state of charge of the battery represented as a value from zero to one. The fuel cell is always on in the light blue area and always off in the dark blue area. The remaining area is a transition area where the fuel cell maintains its on/off state from the previous state that it was in.

The second strategy is an enhanced rule-based strategy and uses similar logic to the mode switching strategy but includes some notable differences. The first is that if the vehicle is braking, the fuel cell ignores the current operating mode and operates at a predefined minimum power set-point. The second is that the battery SOC is now controlled using a target set-point as well as defined upper and lower bounds. If the SOC is above a

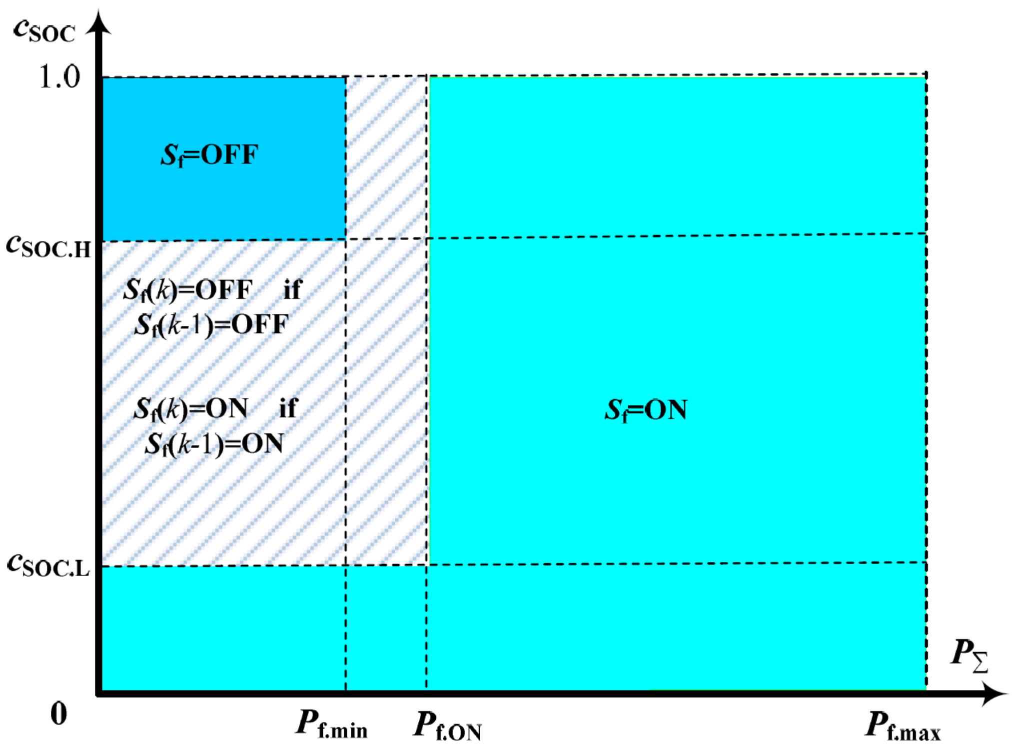

Figure 2.9: Control Logic for the conventional Fuel cell output power oriented Control Strategy [10]

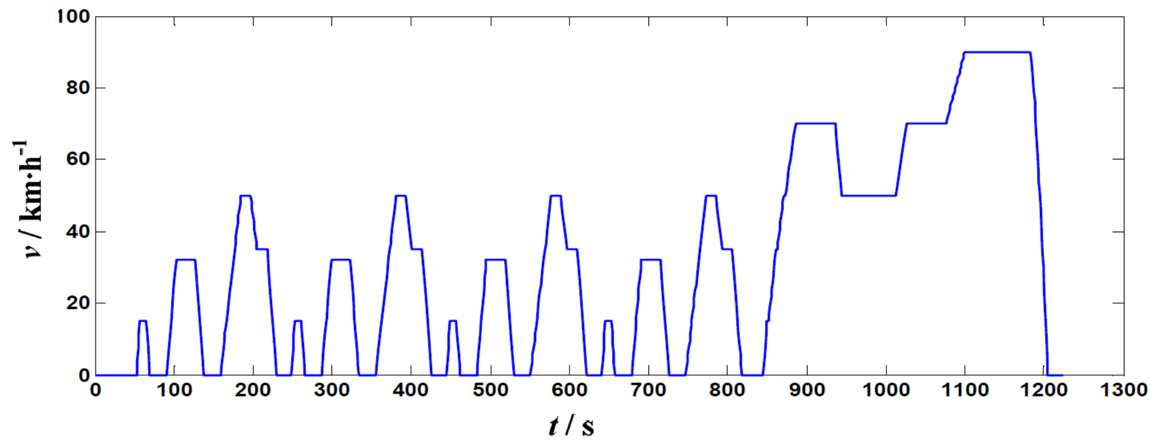

Figure 2.10: Driving cycle for the simulation experiments [10]

	Mode Switching Strategy	Enhanced Rule-Based Strategy
Simulation Results	2.7144 kg/100km	2.5054 kg/100km
Experimental Results	N/A	2.464 kg/100km

Table 2.8: Fuel Cell Powered Bus Results [10]

desired target SOC, the desired battery charging power from the fuel cell is set to zero and the battery discharges slowly based on system transients that cannot be handled by the relatively slow fuel cell. The third is that the fuel cell is now always on in the transition area of Figure 2.9.

The two strategies were tested in simulation on a custom drive cycle as shown in Figure 2.10. Both the mode switching and enhanced rule-based strategies were tested in simulation with the enhanced rule-based strategy showing better results. The enhanced rule-based strategy was then tested on the actual bus. The simulation and experimental results are shown in Table 2.8.

2.4.4 Control of a Fuel Cell Powered Rickshaw

Mallouh et al. studied the effect of different control strategies on the performance of a fuel cell powered auto rickshaw. Using PSAT, a model of a fuel cell powered auto rickshaw

Control Strategy	Fuel Economy	Initial SOC	Final SOC
Fuel Cell Load Following Strategy	1.82 L/100km	60.00%	59.97%
Battery Load Following Strategy	1.88 L/100km	60.00%	58.21%
Fuel Cell Optimized Strategy	1.86 L/100km	60.00%	59.89%
Modified ECMS	1.84 L/100km	60.00%	54.58%

Table 2.9: ECMS Results for Auto Rickshaw Simulation [32]

was developed and four different control strategies were tested in simulation. The rickshaw powertrain is comprised of an 8 kW motor, a 1.5 kWh Li-ion battery system and a 4.4 kW hydrogen fuel cell. The first control strategy tested is a modified ECMS strategy where the cost function, shown in Equation (2.5) is the sum of the power output by the fuel cell added to the adjusted equivalent battery power output. Only one equivalence factor is used and it is directly calculated as a function of the DC/DC converter, fuel cell and battery efficiencies as shown in Equation (2.6).

$$J = P_{FC}^{H2} + P_{batt}^{H2} \tag{2.5}$$

$$s = \frac{\eta_{batt}}{\eta_{FC} \times \eta_{DCDC}} \tag{2.6}$$

The second strategy evaluated is a fuel cell load following strategy where the fuel cell provides the full power demand up to its peak output at which point the battery provides the remaining power. The fuel cell charges the battery when the battery state of charge, SOC, drops below a predefined set-point. The third strategy is a battery load following strategy where the battery provides the full power demand up to its maximum output at which point fuel cell is switched on to provide the remaining power. As with the second strategy, the fuel cell is used to charge the battery when the SOC goes below a predefined set-point. The final strategy evaluated is called the fuel cell optimized strategy and sets the fuel cell to its peak efficiency operating point. The battery manages all transients. When the battery SOC drops below a minimum set-point the fuel cell switches modes and starts charging the battery while also meeting the full power demand. Table 2.9 presents an evaluation of these strategies in simulation for a custom drive cycle. For the auto rickshaw, a fuel cell load following strategy was shown to provide the best fuel economy.

The results presented by Mallouh et al. demonstrate a viable fuel cell control strategy for fuel cell powered rickshaws. Rickshaws, however, have very different dynamics when compared to many other vehicles, such as the vehicle presented in this thesis. Furthermore, the fuel cell system and battery were substantially smaller than the ones used in the test vehicle presented in this thesis and all tests were only performed in simulation without experimental results to validate the performance in real-world applications. It is therefore necessary to test hybrid fuel cell control strategies against other vehicles in order to ensure that these results remain constant for different types of vehicles and to further validate these results with on-road testing.

Chapter 3

Fuel Cell Hybrid Vehicle Testbed

The research presented in this thesis uses a custom built Li-ion fuel cell hybrid vehicle as a test bench. This vehicle is based on a 2009 Saturn Vue and was originally built by the University of Waterloo Alternative Fuels Team (UWAFT) for the three year EcoCAR competition [53]. The author of this work's role on the student team during the EcoCAR competition was that of a controls team member. Primary responsibilities were to develop the hybrid control strategy and the control code necessary to operate the rear motor. This included configuring and tuning the rear motor controller for the specific motor that was used as well as developing supervisory control logic for the vehicle. This also involved assisting with the various electric and mechanical tasks required to build the vehicle including battery pack manufacturing, DC/DC testing, high voltage wiring, cooling system design and various other tasks.

The EcoCAR competition is part of a series of typically three year competitions sponsored by several other organizations involved in the automotive industry [53]. The goal of these competitions is to train students in the skills needed to work in the automotive industry by having them build customized vehicles that incorporate some of the newest and most advanced vehicle technologies currently available. The competition sponsors provide substantial funding and support to the student teams by providing them access to a substantial amount of automotive hardware, software and tools which allows the teams to build technologically advanced, fully functional, road-safe vehicles. Many universities across North America apply to participate in these competitions with only a few being accepted based on the team's available facilities, technical capability and university support. The University of Waterloo has a long history of competing in these competitions and is one of sixteen universities to compete in the EcoCAR competition.

In June 2011, UWAFT completed the three year EcoCAR competition. For this competition, the team built a Plug-in Hybrid Hydrogen Fuel Cell / Li-Ion Battery powered Saturn Vue which placed third of sixteen in the competition. This vehicle was one of only two fuel cell vehicles to participate in the competition and was noted as having excellent drivability with the vehicle just missing first place in the autocross competition by 0.026 seconds. This vehicle was also noted as having a high reliability as the vehicle performed without any hardware or software failures throughout the final competition while performing well in all stress testing events. This combined with the zero tailpipe emissions allowed the vehicle to perform exceptionally well throughout the final competition.

From September to December 2011, this vehicle was used to test control strategies as part of the research outlined in this thesis. In early January 2012, the hydrogen storage tanks from the vehicle were removed and returned to the OEM. In the summer of 2012, the fuel cell stack and front motor were removed and also returned. This vehicle has since been restored as a full electric rear wheel drive vehicle with a new 12 V deep cycle battery bank to provide 12 V power.

This test platform has many advantages. Besides using an industry designed and manufactured fuel cell system that was intended for automotive applications, the fact that the vehicle was developed by the university allows for complete unrestricted access to the vehicle's supervisory control software. This allows for complete freedom in the development and testing of various control strategies without having to bypass any additional software or hardware to enforce the operation of the strategy. The only limitations of this platform are the availability of hydrogen and the return deadline for the hydrogen storage system which limited the amount of testing that could be completed.

3.1 Vehicle Powertrain Architecture

This section provides a detailed description of the test vehicle built by the student team to clearly outline the vehicle architecture which is used in deriving a model of the vehicle used in simulation in Section 3.3.

The powertrain for the Li-ion hydrogen fuel cell hybrid vehicle used in this research is shown in Figure 3.1. The vehicle powertrain is split into two main high voltage electric buses connected together through a Brusa DC/DC converter. The high side of the bus runs at a voltage that is consistently above the 250 V battery system and is comprised of a fuel cell, an electric motor and inverter combination and an integrated 12V DC/DC converter. The low side of the bus runs at a nominal 250 V and is comprised of a 250 V

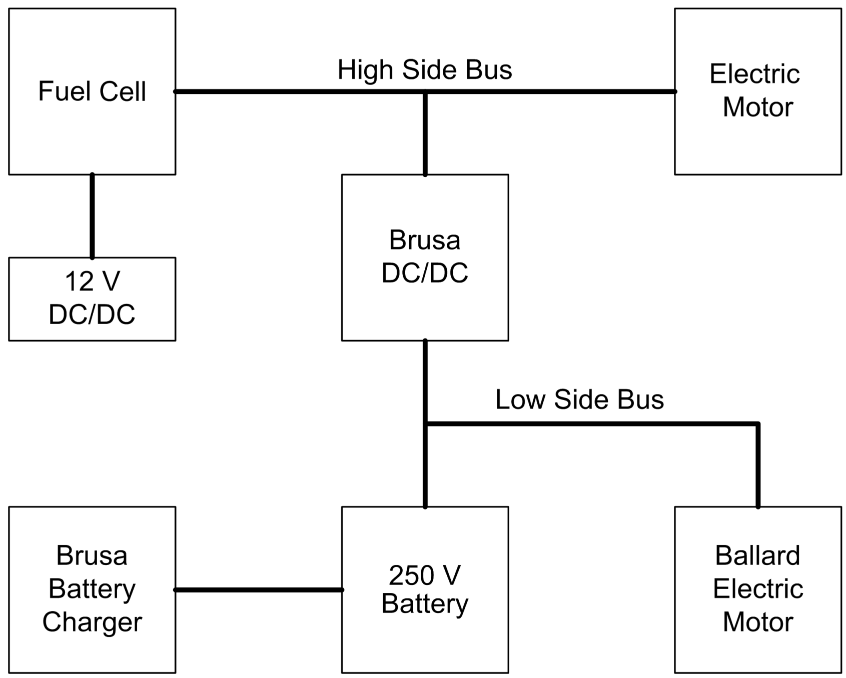

Figure 3.1: Vehicle Powertrain Architecture

battery pack, a Brusa battery charger, a Rinehart inverter and Ballard electric motor. The Brusa DC/DC converter acts as a gateway between the two buses and regulates the power flow in order to allow for charging and discharging of the battery as well as driving the front motor using the battery or the rear motor using the fuel cell. Key operating limits for these components are shown in Table 3.1 where P_{FC} is the fuel cell power output, $P_{FC_{Slew}}$ is the slew rate of the fuel cell power output, P_B is the battery power output, $I_{DC/DC}$ is the current passing through the DC/DC converter, P_{FM} is the power of the front motor and P_{BM} is the power of the rear Ballard motor.

3.1.1 Hydrogen Fuel Cell System

The fuel cell system used in this vehicle was originally developed for a hydrogen fuel cell vehicle program. For the EcoCAR competition, the hydrogen fuel cell system was directly taken from this program so that these systems could be integrated into a 2009 Saturn Vue. The fuel cell system was provided under the agreement that it would be returned at the end of the competition. The donated fuel cell system is comprised of three

Component	Limit
Fuel Cell	$0\,kW \leq P_{FC_i} \lesssim 100\,kW$
	$\lvert P_{FC_{Slew}} \rvert \lesssim 40\,kW$
250 V Battery	$-38\,kW \leq P_{B_i} \leq 98\,kW$
DC/DC Converter	$\lvert I_{DC/DC} \rvert \leq 150\,A$
Front Motor	$\lvert P_{FM} \rvert \leq 110\,kW$
Ballard Motor	$\lvert P_{BM} \rvert \leq 67\,kW$

Table 3.1: Key Component Operating Limits

The hydrogen storage system contains three hydrogen tanks designed specifically for use in automotive applications. Integration of the hydrogen storage system posed a significant challenge. While the tank system was intended to fit within a normal vehicle, the addition of the rear motor to the vehicle architecture resulted in the tank system moving into the passenger cabin and replacing the rear seats.

The fuel cell stack is a proton exchange membrane fuel cell which uses hydrogen and the ambient air to produce electrical energy with water vapour as a byproduct. The fuel cell runs at a peak power output of approximately 100 kW.

Integrated into the fuel cell stack is a 12 V DC/DC converter which takes the power currently on the high voltage bus and converts it into the 12 V power needed for the all the 12 V systems in the vehicle. This power can be sourced from either the fuel cell or the battery. When not active, a small 12 V battery provides the 12 V accessory power to the vehicle which is also required for start up.

3.1.2 Traction System

The vehicle uses a four wheel drive traction system comprised of two electric motors, one for each axle. The front motor is part of the integrated fuel cell system and sits at the bottom of the fuel cell. The front motor has a maximum power output of 110 kW. The rear motor is a Ballard electric traction motor originally sourced from the team's last competition vehicle based on a Chevrolet Equinox. The rear motor has a maximum power output of 67 kW and is powered by a Rinehart PM100 inverter. This motor was rebuilt by the team in order to fix issues with oil leaks and noise. The rear motor suffers from substantial electrical noise issue which required that the motor communication be isolated from the rest of the vehicle and wired directly into the supervisory controller. Additionally, the motor had significant issues with torque shudder which caused the vehicle to shake violently at certain speeds

Figure 3.2: Rear Traction Motor with Subframe[53]

and required a substantial amount of tuning to eliminate. The rear motor and its custom built subframe can be seen in Figure 3.2.

3.1.3 DC/DC Converter

Initially, the vehicle was designed to run with a custom built 110 kW bidirectional buck-boost DC/DC converter designed by the student team. This DC/DC converter would be built by one of the student team's graduate students as a PhD research project. Unfortunately due to time constraints and issues with getting the DC/DC converter to work reliably, the custom DC/DC converter was dropped and replaced with an off the shelf DC/DC converter provided by Brusa and purchased with money donated by Natural Resources Canada. The Brusa DC/DC converter is shown in Figure 3.3. The DC/DC converter used is a BDC412 bidirectional DC/DC converter with dedicated high and low sides as opposed to dynamically switching sides supported by the custom DC/DC converter. This DC/DC converter is used to connect the battery and fuel cell high voltage buses and regulates power flow between the two high voltage systems.

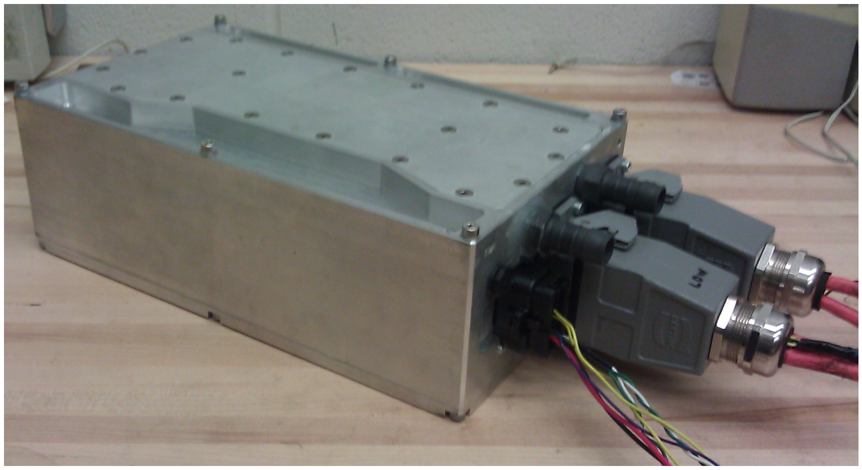

Figure 3.3: Brusa DC/DC Converter

3.1.4 Energy Storage System

The energy storage system is comprised of two major components, a Brusa NLG513-Sx battery charger and a 250 V battery pack. The Brusa charger is shown in Figure 3.4 and is used to add plug-in charging capability to the vehicle's battery system. The Brusa charger directly communicates with the battery using CAN.

The battery pack, shown in in Figure 3.5, is a lithium ion battery pack and functions as the high voltage energy storage system for the vehicle. The battery provides power to the two electric motors and the 12 V DC/DC Converter. The battery can operate with or without the fuel cell system being enabled, allowing for an electric only operating mode as well as a full hybrid mode.

3.1.5 CAN Bus Communication System

The main method of communication used to coordinate the operation of the various components in the vehicle is the CAN Bus. The vehicle's CAN bus architecture is comprised of seven separate CAN buses. Figure 3.6 shows a simplified diagram of this CAN bus architecture with the standard GM controllers and sensors reduced to single nodes.

At the center of the CAN bus is the dSPACE MicroAutoBox (MABX) which acts as the supervisory controller for the vehicle. The vast majority of the high level control logic written by the various members of the team is running on this hardware. The four CAN

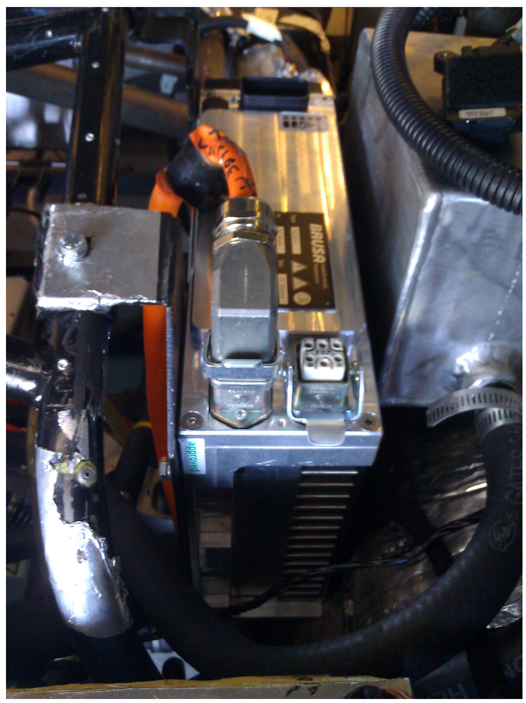

Figure 3.4: Brusa Charger[53]

Figure 3.5: 250 V Battery Pack[53]

buses the MABX interfaces with are the only CAN buses that need to be directly controlled in order to operate the vehicle.

PTECAN is the powertrain expansion bus and is part of the original vehicle as is the Single Wire GMLAN CAN bus. High Speed GMLAN is also part of the original Saturn Vue CAN bus architecture. This CAN bus originally controlled the various components of the stock vehicle. Much of the functionality of this CAN bus has been removed and replaced with the functionality of the new buses. The original signals transmitted by these now missing components are being replicated by the MABX. The main use of this bus is to interface with the Body Control Module (BCM) and read various vehicle sensors while maintaining important stock vehicle functionality such as the ability to use the original vehicle starting system, locks, power windows, lights and gauges.

Fuel Cell CAN is the CAN bus used by the MABX to control the fuel cell both during start up and normal operation. Control is primarily handled by sending power requests to the fuel cell system (FCS) which will cause the fuel cell's internal controller to manage the various internal components of the fuel cell as well as communicate with the hydrogen safety controller to produce the appropriate amount of power. These components will also read the hydrogen sensors which are also located on the CAN bus and automatically shut down when a serious hydrogen leak is detected. The fuel cell system communicates with a

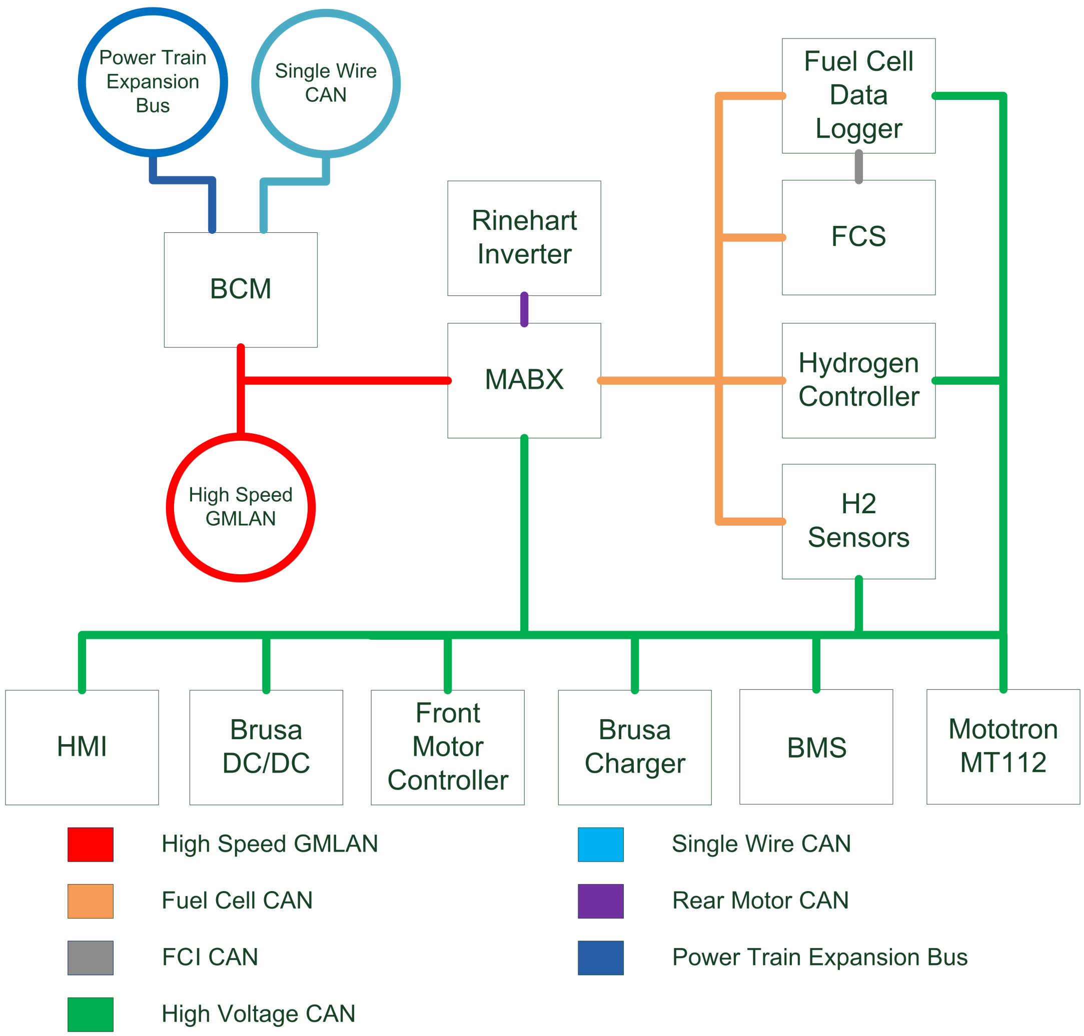

Figure 3.6: CAN Bus Architecture

data logging system through the FCI CAN bus.

High Voltage CAN is used to manage the high voltage battery system and related components in the vehicle. The BMS is the controller for the battery system. It is primarily used to report the battery status to the rest of the vehicle. The front traction motor has its own controller which is controlled through CAN by the MABX. The Human Machine Interface (HMI) is a dash mounted display that is used to report key vehicle operating parameters to the driver. This includes vehicle operating mode, diagnostics, battery state of charge and voltages for both the high a low voltage batteries. The Mototron MT112 is a secondary controller which runs software developed by the team to directly supply power to pins on various hardware components based on commands received from the MABX. The Mototron was used to address current draw limitations that exist within the MABX hardware.

The Rinehart inverter has its own CAN bus called Rear Motor CAN. This bus is used to control the rear motor and was implemented as a separate bus to address noise issues caused by the inverter when it was originally placed on the High Voltage CAN bus. Commands are sent directly from the MABX.

3.2 Vehicle Software Architecture

The MABX is used as the supervisory controller for the vehicle. All high level decision making is done here. The MABX code is written using Simulink. At the highest level the control code is broken into three sections which interface with the sensing and actuation systems of the vehicle as shown in Figure 3.7.

3.2.1 Diagnostic Subsystem

The first section is the Diagnostics subsystem. This subsystem is responsible for detecting component failures and setting component state control flags which indicate the current operating mode of the individual hardware components. The detected failures and component flags are used later in the code to inform the high level control code about any issues or commands to which it must respond and to facilitate switching vehicle operating modes.

The diagnostic code is divided up into eight subsystems based on the individual powertrain components. These diagnostic subsystems are listed below:

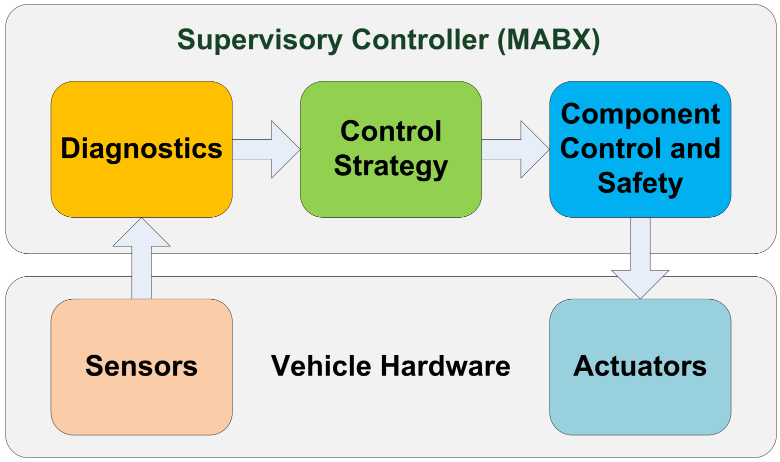

Figure 3.7: MABX Software Architecture Overview

- Fuel Cell Stack
- 250 V Battery System
- Brusa DC/DC
- Brusa Hydrogen Storage System
- Brusa Front Traction Motor
- Brusa Rear Traction Motor
- Brusa Brusa Charger
- Brusa Vehicle

3.2.2 Component Control and Safety Subsystem

The Component Control and Safety subsystem is responsible for managing the vehicle state machine and reinterpreting the decisions made by the control strategy subsystem into signals that can be directly sent out onto the CAN bus to the other components of the vehicle. The vehicle state machine contains a Simulink Stateflow diagram that manages the highest level of operating state for the vehicle. An overview of the Stateflow diagram is shown in Figure 3.8.

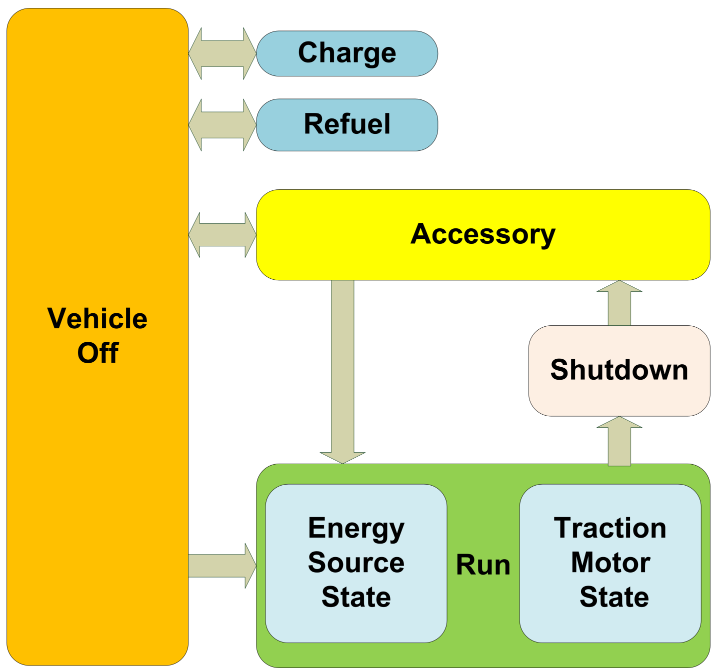

Figure 3.8: Vehicle State Machine

The vehicle state machine manages the start up and shutdown sequencing for the vehicle and is responsible for responding to any serious system failures in the vehicle by either reverting to an electric only operation, disabling one of the two traction motors or shutting off the vehicle. The Run state is subdivided into two parallel Stateflow diagrams. The first is called the Energy Source State which manages the start up, shut down and failure modes for the main energy source components including the Fuel Cell System, Battery and DC/DC converter. This logic is also responsible for enabling or disabling full hybrid operation as selected by the driver using the hybrid mode enable switch. The second state flow diagram is called the traction motor state and is responsible for enabling and disabling motors based on the state of the motors and power sources.

3.2.3 Control Strategy Subsystem

The Control Strategy subsystem contains the main decision making algorithms for the high level operation of the vehicle's powertrain. This system is divided into three major subsystems. These subsystems are thermal control, torque control and hybrid control.

Thermal Control

The thermal control subsystem is responsible for managing the temperatures of all the main powertrain components. This is accomplished by enabling or disabling the various fans and pumps that are part of the vehicle's cooling systems. This system operates using thermostat control logic, enabling pumps when the temperature of a component in the loop exceeds a certain threshold and enabling fans when an even higher threshold is exceeded. A small hysteresis in the temperature thresholds exists between the on/off operation of the pumps and fans in order to prevent rapidly cycling the pumps and fans.

Torque Control

The Torque Control subsystem is responsible for controlling the vehicle's traction subsystem which is comprised of the two motor/inverter systems.

The torque control strategy processes the driver's torque request by using the accelerator pedal map which is given in Figure 3.9. If the brakes have been engaged then the resulting torque from the pedal map is set to 0. This is to prevent the driver from trying to demand positive acceleration torque while also pressing down on the brake pedal.

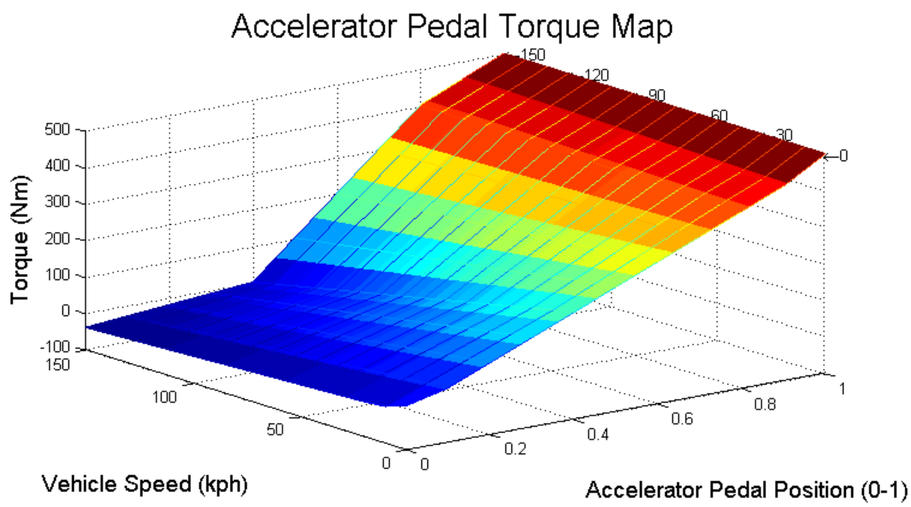

Figure 3.9: Accelerator Pedal Map

The brake pedal position is also used to calculate the regenerative braking request. This is calculated using Equation (3.1), where B_{Pos} is the break pedal position as a fraction from 0 to 1, T_{Regen} is the regenerative braking torque requested in Nm, and v_{veh} is the vehicle speed in kph. K is a scaling factor set to 250 to produce torque from the brake pedal position and the vehicle speed. The value of K was selected through extensive testing.

$$T_{Regen} = B_{Pos} \times K \times (v_{veh} - 10) \tag{3.1}$$

Regenerative braking is set to 0 at speeds under 10 km/h and when the regenerative braking disable switch is engaged. In this situation all braking is done using the mechanical braking system.

The acceleration and braking demands are processed using the motor torque splitting algorithm which takes the desired torque and splits it between the two motors based on the desired torque split ratio and the motor power limits.

The desired torque split is set to a constant 30% rear and 70% front. As the vehicle's motor torque demand approaches the limits of the front motor, the vehicle shifts the torque split putting a greater percentage of the torque demand on the rear motor to protect the front motor from exceeding its power limit.

Hybrid Control

The hybrid control subsystem is responsible for managing the high level control of the vehicle energy sources. This includes the 250 V battery, the fuel cell and the Brusa DC/DC Converter. Several different control strategies have been implemented as part of the research detailed in this thesis. These strategies are described in detail in Chapter 4.

The hybrid control subsystem reads in the power requested by the front and rear motors and then calculates the desired amount of fuel cell power that must be provided based on the current control strategy logic. The fuel cell power is then read by the DC/DC control subsystem which determines the voltage set points for the DC/DC required to provide the remaining requested power from the battery. In the process, all decisions made on the power set-points are validated against the safe operating limits of the components.

3.3 Vehicle Model

To test various different control strategies, a simulated model of the vehicle has been developed in Matlab. The vehicle model used in simulation is a powertrain model which relates the changes in battery state of charge (SOC) and hydrogen consumption to the power output of the fuel cell and battery.

The fuel cell model assumes a constant temperature. Equation (3.2) is defined as the fuel map equation which was determined through on-road testing. Equation (3.2) forms the basis of the fuel cell model. The equation that defines the amount of hydrogen consumed as a function of the fuel cell power is represented by $m\left(P_{FC}\right)$.

$$m\left(P_{FC}\right) = 9.65 \times 10^{-11} \times P_{FC}^{2} + 1.38 \times 10^{-5} \times P_{FC} + 3.29 \times 10^{-2} \tag{3.2}$$

A plot of the fuel cell stack efficiency as for the model of the fuel cell is shown in Figure 3.10, where it can clearly be seen that the fuel cell operates at peak efficiency in the 10 to 20 kW region. Outside this region, the fuel cell efficiency starts to drop off.

The DC/DC converter efficiency is approximately 97%. This value was provided by the data sheet from the manufacturer and is represented in the following equations as $\eta_{DC/DC}$.

The battery model assumes constant temperatures. Nonlinearities in power transfer in or out of the battery pack are included as part of the battery efficiency. The electrical efficiency, η, is calculated using Equation (3.3) when the battery is being charged and Equation (3.4) when the battery is being discharged.

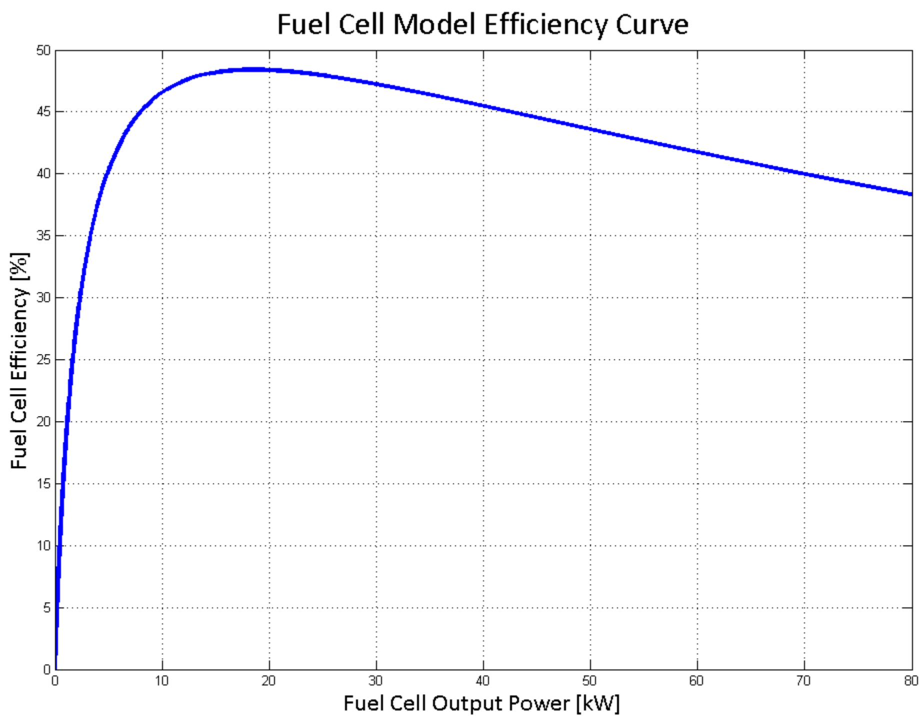

Figure 3.10: Simulated Fuel Cell System Efficiency Curve

$$\eta = \eta_B \times \eta_{DC/DC} \qquad I < 0 \tag{3.3}$$

$$\eta = \frac{1}{K_s \times \eta_B + (1 - K_s)\, \eta_{Batt} \times \eta_{DC/DC}} \qquad I > 0 \tag{3.4}$$

The battery efficiency, η_B, has been measured to be fairly static at approximately 97.55%. This battery efficiency was calculated by matching experimental data to the model and minimizing the prediction error. K_s is the percentage of the power output consumed by the rear motor and is set to 30%. This value can change throughout the drive cycle as the torque controller has the capability of dynamically shifting torque to adjust for component limits such as the DC/DC converter current limit and the motor torque limits.

The battery SOC is modeled using Equation (3.5) where SOC is the battery state of charge as a percentage, η, is the efficiency of energy going into and out of the battery, as defined in (3.3) and (3.4), I is the current output by the battery and Q is the capacity of the battery and is set as 40 Ah.

$$SOC_t = SOC_{t-1} - \frac{I \times \eta \times dt}{Q \times 3600} \times 100 \tag{3.5}$$

3.3.1 SOC Adjusted Fuel Economy

The fuel economy of a vehicle is typically calculated using the fuel mass consumption of the given driving mission and the distance traveled. For hybrid vehicles, this calculation becomes slightly more complicated, as it is necessary to also account for the net change in the battery state of charge over the drive cycle. Since the final state of charge of the battery can vary, depending on the strategy used, the fuel economy numbers can become skewed. To account for changes in the battery SOC, an SOC adjusted fuel economy is used. Four methods of calculating the fuel consumption have been considered. These include a fuel only calculation, a power adjusted fuel map method, an optimal charge/discharge method and an averaged charge/discharge method.

Fuel Only

The fuel only calculation ignores the deviation in the battery charge. This approach assumes the deviation to be minor and calculates the fuel economy using only the fuel map provided in Equation (3.2). The fuel consumption calculation is given in Equation (3.6) where M is the total fuel consumption and n is the final time step of the simulation or experiment.

$$M = \sum_{i=1}^{n} \left[m\left(P_{FC_i}\right) \right] \tag{3.6}$$

The fuel consumption calculated using this method completely ignores the battery energy usage which makes it impractical for use on hybrid vehicles. This approach favours completely discharging the battery and is expected to show inaccurate results for cases where the SOC of the battery changes substantially at the end of the drive cycle.

Power Adjusted Fuel Map

The power adjusted fuel map method attempts to recalculate the fuel consumption of the fuel cell so that the battery state of charge at the end of the cycle matches the initial battery state of charge. The amount of power required to charge or discharge the battery is calculated using Equations (3.7) and (3.8).

$$\triangle SOC = \frac{SOC_1 - SOC_n}{100\%} \tag{3.7}$$

$$P_{SOC} = \frac{Q \times 3600 \times \triangle SOC \times V}{\eta \times dt} \tag{3.8}$$

This power is then added to the power output of the fuel cell using Equation (3.9) to get the adjusted fuel cell power demand, P_{adj_i}.

$$P_{adj_i} = P_{FC_i} + \frac{P_{SOC}}{n} \tag{3.9}$$

The fuel consumption is calculated using Equation (3.10).

$$M = \sum_{i=1}^{n} \left[m\left(P_{adj_i}\right) \right] \tag{3.10}$$

When P_{SOC} is negative and the fuel cell power output is sufficiently low, this approach allows for the value of the adjusted fuel cell power to dip below the idle fuel consumption of the fuel cell and potentially result in an instantaneous fuel consumption that is negative. This is valid since this comes as a result of energy being stored in the battery from consuming fuel at other points in the drive cycle the total fuel consumption calculated using this method will always return positive values for all simulations and tests performed as part of this research.

Optimal Charge/Discharge

The optimal charge/discharge method calculates the fuel consumption from the fuel only method given in Equation (3.6) and adds or subtracts the equivalent fuel for the battery state of charge deviation based on the optimal operating point of the fuel cell. The equivalent battery fuel is calculated using Equation (3.11).

$$m_B = m\left(P_{FC}^*\right) \times \frac{P_{SOC}}{P_{FC}^*} \tag{3.11}$$

The fuel consumption is then calculated using the fuel cell fuel consumption calculated in Equation (3.6) and Equation (3.12).

$$M = m_{FC} + m_B \tag{3.12}$$

Averaged Charge/Discharge

The averaged charge/discharge method is almost identical to the optimal charge/discharge method. The only difference is that instead of basing the equivalent fuel usage on the optimal efficiency point of the fuel cell, this approach uses the average power output of the fuel cell over the full drive cycle. The average fuel cell power output is calculated in Equation (3.13).

$$P_{FC_{avg}} = \frac{\sum_{i=1}^{n}\left(P_{FC_i}\right)}{n} \tag{3.13}$$

The equivalent fuel for the battery is calculated using Equation (3.14).

$$M_B = m\left(P_{FC_{avg}}\right) \times \frac{P_{SOC}}{P_{FC_{avg}}} \tag{3.14}$$

The fuel consumption is then calculated using the fuel cell fuel consumption calculated in Equation (3.6) and Equation (3.12) as before.

Since SOC deviations can introduce a significant amount of error when calculating fuel economy each of the above methods are discussed in the results presented in Chapter 5, in order to demonstrate a proper comparison between the various strategies being evaluated.

Fuel Economy Calculation

Once the equivalent hydrogen fuel consumption is calculated using one of the above methods it must be converted into an equivalent measurement in miles per gallon of gasoline. This is done by multiplying the fuel economy measured in miles driven per kilograms of hydrogen consumed by a scaling factor, K_H as shown in Equation (3.15) where D is the distance driven. The value of K_H is defined as 0.98 and is taken from the EcoCAR competition guidelines.

$$FuelEconomy = \frac{D}{M} \times K_H \tag{3.15}$$

Chapter 4

Controllers

Once the vehicle model has been properly defined, the specific control strategies to be tested can be developed. In this thesis, three main control strategies are tested and evaluated against an optimized solution. The three strategies evaluated are a mode switching rule-based strategy, a constant fuel cell output strategy and an adaptive equivalent consumption minimization strategy. To begin evaluating these strategies, the full control problem must first be defined.

4.1 Problem Statement

At its most basic level, hybrid vehicle control comes down to satisfying the vehicle power demand, P_D, as shown in Equation (4.1) where P_B is the power provided by the battery.

$$P_D = P_{FC} + P_B \tag{4.1}$$

This equation states that at any given time, the power coming from the battery and the fuel cell must equal the vehicle power demand as commanded by the driver based on the current position of the brake and accelerator pedals as well as the current vehicle speed. Equation (4.1) must be satisfied in order for the vehicle to be considered drivable and as such is considered a hard constraint on the vehicle's operation, secondary only to the operating limitations of the components and the safety requirements for the vehicle. This also means that the fuel consumption of the vehicle is solely dependent on the ratio of P_{FC} and P_B throughout the entire drive cycle. Ideally, P_{FC} and P_B would be selected so as to also minimize the overall fuel consumption of the vehicle and maximize fuel economy over the drive cycle. Determining how to set the power levels P_{FC} and P_B to minimize fuel consumption while satisfying power demand is where the challenge lies in hybrid vehicle control.

4.2 Optimal Power Split

With prior knowledge of the vehicle's power demand, determining the best possible fuel economy for a given drive cycle can be achieved by formulating the power split problem as a quadratic programming optimization problem. The cost function is given directly as the fuel map for the fuel cell since this provides the most direct measurement of fuel consumption without introducing any inaccuracy or bias towards a strategy that unfairly favours charging or discharging the battery [48] This optimization is formulated in Equations (4.2) through (4.11) which restate the model of the hybrid fuel cell vehicle defined in Chapter 3.

minimize:

$$J = \sum_{i=1}^{n} \left[m\left(P_{FC_i}\right) \right] \tag{4.2}$$

subject to:

$$P_{D_i} - P_{FC_i} - P_{B_i} = 0 \qquad i = 1, ..., n \tag{4.3}$$

$$0 \leq P_{FC_i} \lesssim 100000 \qquad i = 1, ..., n \tag{4.4}$$

$$\left| P_{FC_i} - P_{FC_{i+1}} \right| - P_{FC_{Slew}} \leq 0 \qquad i = 1, ..., n \tag{4.5}$$

$$SOC_i - SOC_{i-1} + \frac{I_i \times \eta \times dt}{Q \times 3600} \times 100 = 0 \qquad i = 2, ..., n \tag{4.6}$$

$$-38000 \leq P_{B_i} \leq 98000 \qquad i = 1, ..., n \tag{4.7}$$

$$40 \leq SOC_i \leq 60 \qquad i = 1, ..., n \tag{4.8}$$

$$SOC_I - SOC_1 = 0 \tag{4.9}$$

$$SOC_I - SOC_n = 0 \tag{4.10}$$

$$\left| I_{DC/DC_i} \right| \leq 150 \qquad i = 1, ..., n \tag{4.11}$$

The cost function is given as J, SOC_i is the state of charge of the battery at a given time and SOC_I is the initial SOC of the battery. The optimization is constrained such that the battery's state of charge is bounded between 40 and 60 percent and is also fixed to a desired final value. For simulation, this value is selected to be the initial state of charge which is set to 50 percent.

While performing the above optimization gives the solution that provides the best possible fuel economy, it requires that the drive cycle's power demand profile be completely known prior to starting the drive cycle. It is, however, not possible to know the power demand in advance for normal driving conditions, as the driver initiates the requests while driving based on traffic and road conditions. As such, this approach is not usable on real vehicles and is only useful as a benchmark in simulation to determine the effectiveness of other control strategies.

4.3 Rule-Based Strategies

Rule-based strategies are strategies that use a series of rules to define their operation based on the current state of the vehicle's operation. Rule-based strategies do not include advanced learning or prediction methods which can be used to tune the operation of the strategy. These strategies are used on most current hybrid vehicles such as the Toyota Prius [20]. The advantage of rule-based strategies is that they are simple to implement, consistently causal and easy to test. The following two strategies were tested on the vehicle in real world implementations as well as in simulation.

4.3.1 Mode Based Control

The idea of this strategy is to run the vehicle in several different operating modes based on battery SOC and vehicle power demands. The goal is to keep the battery SOC between an upper, SOC_{UB}, and lower, SOC_{LB}, bound. The region defined by these bounds should be low enough to take full advantage of the battery capacity while still allowing for some room below the bounds in the event that the driver requests a significant amount of power from the vehicle while the SOC is relatively low. The bandwidth defined by the bounds only needs to be large enough to prevent aggressive braking and acceleration events from causing the vehicle to continually hit the bounds and repeatedly switch operating modes. This strategy operates in three distinct modes as shown in Table 4.1 where $P_{discharge}$ is a constant discharging set point for the battery and P_{charge} is a constant charging set point for the battery. These modes are Discharge, Sustain and Charge. Component safety code also exists which is used to protect DC/DC convert and the fuel cell from exceeding their

Mode	Entry Condition	Operating Points
Discharge	$SOC \geq SOC_{UB}$	$P_{B_i} = P_{D_i}$
		$P_{FC_i} = 0\,kW$
Sustain	$SOC_{LB} < SOC \leq SOC_{UB}$	$P_{B_i} = P_{discharge}$
		$P_{FC_i} = P_{D_i} - P_{discharge}$
Charge	$SOC \leq SOC_{LB}$	$P_{B_i} = P_{charge}$
		$P_{FC_i} = P_{D_i} - P_{charge}$

Table 4.1: Rule-Based Control Strategy Operating Modes

current and power limits respectively. This code detects when requests from the mode based control approach the limits of the components as specified in Table 3.1 and shifts the power split to stay within the safety limitations of the vehicle powertrain.

4.3.2 Constant Fuel Cell Output

The constant fuel cell output strategy is a simple control strategy which was inspired by the realization that the difference between peak fuel cell efficiency and off peak is notably larger than the storage losses in the battery. The relatively small loss in round trip power storage and consumption from the battery is more efficient than all but a small band of fuel cell operating points near the peak efficiency point of the fuel cell. As a result, keeping the fuel cell at near constant power output and using the battery to satisfy instantaneous power demand is a promising rule-based strategy. This rule-based strategy sets the fuel cell output to the average power demand expected for the drive cycle. The battery acts as a buffer and handles all the transients. Due to the sizing of the fuel cell for the test vehicle, this set point is close to the optimal operating point of the fuel cell for the drive cycles that have been tested. This is not necessarily true for all drive cycles as some cycles may have very low or high power demands or extensive idling time. Each of the tested cycles represent typical driving patterns for the average driver and as such it is expected that a properly sized fuel cell for any vehicle should operate near its optimal operating point under normal operation for the average driver. This strategy is very simple computationally and should also be able to improve the fuel economy over the mode based strategy.

4.4 Equivalent Consumption Minimization Strategy

As part of the research presented in this thesis, a variation of the Adaptive Equivalent Minimization Strategy (A-ECMS) capable of running on a fuel cell vehicle has been developed. To create a fuel cell variation of the A-ECMS strategy it is first necessary to generalize the Equivalent Consumption Minimization Strategy (ECMS) so that the fundamental principles of the ECMS can be implemented in the modified A-ECMS.

The ECMS strategy was earlier introduced in Chapter 2 and was developed primarily for use in hybrid electric vehicles with an internal combustion engine as a way of optimally selecting the power split based on the current state of charge of the vehicle's battery. The goal of the strategy is to reduce the complexity of the optimization problem to an optimization that can be run in real time on the vehicle with minimal knowledge of the future power demand [11]. This is accomplished by formulating an equivalent fuel consumption calculation for the energy that is consumed from the battery and relating it to changes in the state of charge of the battery. The new cost function for the optimization becomes a function of the engine's fuel map and the equivalent battery fuel map. This map is based on the fuel map of the engine. The value of battery power however, depends on the drive cycle and the resulting changes in battery SOC throughout the vehicle's operation [11]. To use a generic equivalent battery fuel map the battery power must be adjusted to it's equivalent value for the current drive cycle. The equivalent battery power is formulated using Equation (4.12) where s is called the equivalence factor.

$$P_{B_{Eq}} = s \times P_B \tag{4.12}$$

This equivalence factor is dependent on changes in the battery state of charge over the expected drive cycle. Each drive cycle has two equivalence factors, one for charging the battery and one for discharging the battery. The calculation of these factors is discussed in detail in [4, 19].

To adapt the ECMS for use on a fuel cell vehicle, the fuel cell fuel map must replace the engine fuel map in the cost function and the equivalence factors must be adjusted according to the new vehicle architecture. The new equivalence factors used are based on the adaptive equivalent minimization strategy discussed in the next section.

Since the power stored in the battery is primarily produced by the engine, the equivalent fuel consumed by the battery, m_B, is calculated by taking the peak efficiency fuel consumption of the fuel cell and linearly scaling it based on the equivalent battery power as shown in Equation (4.13).

$$m_B = P_{B_{Eq}} \times \frac{m\left(P_{FC}^*\right)}{P_{FC}^*} \tag{4.13}$$

The optimization problem for the ECMS strategy is defined in Equations (4.14) through (4.21) where $P_{FC_{i-1}}$ and SOC_{i-1}represent the fuel cell power and battery SOC from the optimization for the last time step. The fuel cell power from the last time step is initialized to 0 and the SOC is initialized to SOC_I for the first optimization.

minimize:

$$J_i = m\left(P_{FC_i}\right) + m_{B_i} \tag{4.14}$$

subject to:

$$P_{D_i} - P_{FC_i} - P_{B_i} = 0 \tag{4.15}$$

$$0 \leq P_{FC_i} \lesssim 100000 \tag{4.16}$$

$$\left|P_{FC_{i-1}} - P_{FC_i}\right| - P_{FC_{Slew}} \leq 0 \tag{4.17}$$

$$SOC_i - SOC_{i-1} + \frac{I_i \times \eta \times dt}{Q \times 3600} \times 100 = 0 \tag{4.18}$$

$$-38000 \leq P_{B_i} \leq 98000 \tag{4.19}$$

$$40 \leq SOC_i \leq 60 \tag{4.20}$$

$$\left|I_{DC/DC_i}\right| \leq 150 \tag{4.21}$$

Note that this optimization does not depend on any future time steps and as such is much simpler and faster to compute. In order for this optimization to work it is still necessary to have the two equivalence factors which are directly dependent on the drive cycle [11]. To implement the ECMS optimization, it is necessary to find a way of determining the equivalence factors without directly knowing the drive cycle. Several variations of the ECMS have been developed to overcome this issue, including a telemetry based ECMS and an adaptive ECMS [19]. The adaptive ECMS is discussed in more detail in the following section.

4.4.1 Adaptive Equivalent Consumption Minimization Strategy

The Adaptive Equivalent Consumption Minimization Strategy (A-ECMS) was also introduced in Chapter 2. This section describes how the A-ECMS strategy is adapted for use

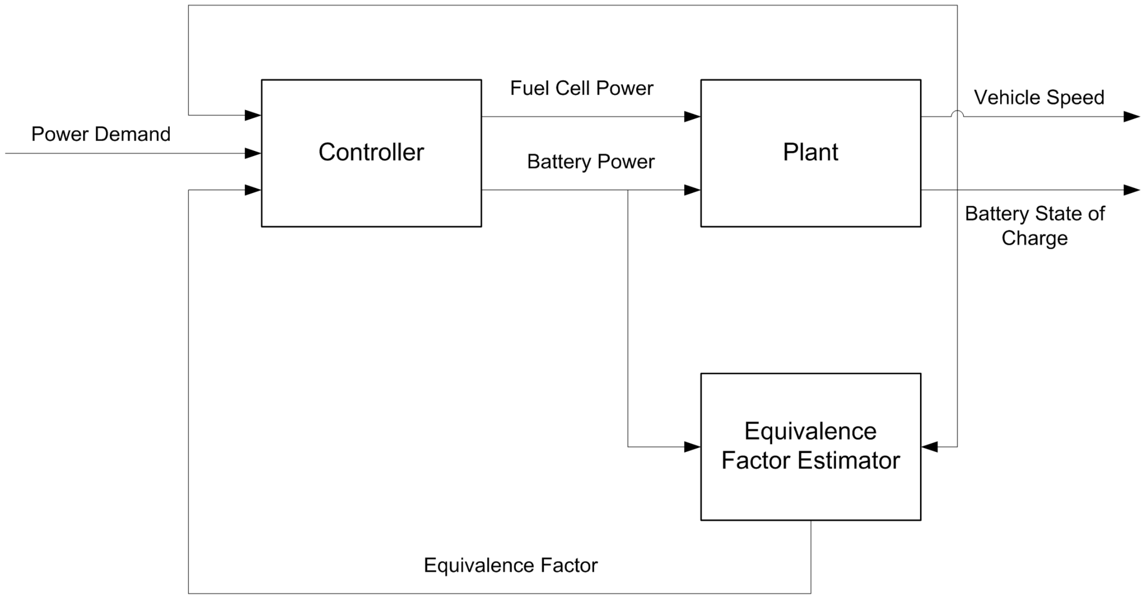

Figure 4.1: Control Layout for Adaptive Equivalent Consumption Minimization Strategy Implementation

on the test vehicle.

The way A-ECMS works is that it takes the ECMS and simplifies it by reducing the two equivalence factors to a single factor and then adjusting this factor in real time [11]. This is done by generating an estimate of the vehicle's power demand throughout the driving mission and producing an estimate of the equivalence factor in order to maintain a desired battery SOC range. The approach proposed by Musardo uses the velocity profile of the vehicle and the elevation provided by GPS data to predict the road load of the vehicle for the duration of the driving mission [11]. The approach used in the simulations presented in this paper takes the average power demand of the drive cycle and an estimate of the end time of the mission and uses this to predict deviations in the battery SOC from an ideal desired value. The equivalence factor is adjusted to compensate for these deviations by reacting proportionally to the error in SOC relative to the desired SOC set point. A block diagram of the adaptive control structure is given in the Figure 4.1.

To adjust the equivalence factor, the average current going into the battery since the start of the mission is calculated. This average current gets propagated forward using an estimate of the end time of the mission and the model of the battery given in Equation (3.5) to determine an estimated final state of charge as shown in Equation (4.22) with the error, e, given by Equation (4.23). The end time of the mission can be estimated using GPS navigation software or recorded past driving mission times which can be cross-referenced with the current day of the week and time to get an estimate of the driving time for the current mission. For the simulations presented in this thesis, the end time is taken as the actual end time of the drive cycle.

$$SOC_{n_{est}} = SOC_i + \frac{I_{avg} \times \eta \times dt}{Q \times 3600} \times (n - i) \times 100\% \tag{4.22}$$

$$e = \frac{SOC_{n_{des}} - SOC_{n_{est}}}{100} \tag{4.23}$$

The $SOC_{n_{des}}$ term is the final desired SOC and $SOC_{n_{est}}$ is the estimated final SOC. I_{avg} is the average battery current over the current drive cycle. The adaptive estimation of the equivalence factor is then calculated using Equation (4.24) where K is the adaptive gain and must be determined through experimentation or simulation.

$$s_i = s_{i-1} + K \times e \tag{4.24}$$

Based on simulation, a value of 0.005 per second for K has been selected. This value provides a good balance between allowing the SOC to drift which provides some freedom in controlling the fuel cell power output and ensuring the battery state of charge does not drift close to its safety limits. The calculation in Equation (4.24) is done at each time step prior to calculating the optimal solution. Once the equivalence factor has been determined it is used in Equation (4.12) to determine $P_{B_{Eq}}$ and the optimization problem for the ECMS strategy defined in Equations (4.14) through (4.21) is solved.

Chapter 5

Results

Five controllers have been presented in the previous chapter. The optimal controller is the first controller presented and provides the best possible fuel economy that can be achieved on the vehicle. The optimal controller is only usable in simulation because the entire drive cycle power demand must be known in advance. The optimal controller is therefore used exclusively to provide a benchmark for all other strategies to be measured against. Two rule-based strategies have also been presented. These strategies include a mode based control strategy that switches between three different algorithms to maintain the battery state of charge between an upper and lower bound and a constant fuel cell output strategy that keeps the fuel cell output near its peak efficiency based on the average power required by the vehicle. Both strategies are implementable in both simulation and experimental tests with the constant fuel cell strategy promising to show very efficient results. An ECMS has been presented which promises near optimal fuel economy results. The main drawback for the ECMS is that it requires accurate equivalence factors be determined for each drive cycle prior to driving through the cycle and is not directly compatible with the fuel cell architecture. Rather than implement this strategy directly, the final strategy that has been presented is an A-ECMS that has been modified to operate on a fuel cell vehicle. This strategy promises to show near optimal fuel economy results, similar to the ECMS, but uses a different prediction method that is not directly dependent on the vehicle architecture which makes it more practical for implementation in simulation. Some knowledge of future parameters is still needed by the A-ECMS which makes implementation on a vehicle still challenging. Each of the proposed controllers, with the exception of ECMS, were investigated in simulation with the two rule-based strategies also investigated in on-road testing. The results of these simulations and experiments are described in the following sections.

5.1 Simulation Results

Simulations of the various controllers have been performed on several drive cycles, including UDDS, HWFET and US06. Based on experimentation with the test vehicle, it was determined that the bandwidth defined by the SOC bounds for the mode switching strategy can be as little as one or two percent of the SOC. The SOC limits were therefore set to 51% and 49% for the upper and lower bounds respectively as used in Table 4.1 while $P_{discharge} = 15kW$ and $P_{charge} = -15kW$ were selected as the charge and discharge constants. Power split and fuel economy results are presented for each type of controller on all three drive cycles, and reveal remarkably consistent results.

5.1.1 Fuel Economy Results

Four different fuel economy measurement methods have been evaluated, as described in Section 3.3.1, to determine an appropriate way of adjusting the vehicle fuel economy to accommodate for deviations in the battery state of charge. Table 5.1 presents the final state of charge for each simulation. In all cases, the SOC deviations are less than 2%. Tables 5.2, 5.3, 5.4 and 5.5 present the simulation results for the various different SOC adjustment methods. As can be seen from Table 5.2, not taking the SOC deviations into account makes it impossible to compare the results from the different strategies. In two cases, the fuel economies of the different strategies exceed the fuel economy reported as the optimal value. This indicates that in order to properly compare these results it is necessary to consider the extra power stored or discharged by the battery when determining the effectiveness of a strategy. The power adjusted fuel map, optimal charge / discharge and averaged charge / discharge weighting methods shows similar results with the same general trends in terms of which strategies provide better results. Most importantly, all the results indicate that the optimal solutions have the best fuel economy which is a requirement for these methods to be considered valid. The consistency of these results indicates that all three of these methods are effective at accounting for the deviation in the state of charge of the battery. These results are expected since the deviations in SOC are relatively minor which makes it difficult to distinguish the differences between the methods.

One interesting note is that there is very little difference in the fuel economies between the different control strategies for each drive cycle. The largest difference in fuel economy is only 3.51 mpg. It is very clear, however, that the mode based strategy and A-ECMS are not as efficient as the constant fuel cell strategy which can achieve consistently higher fuel economy results.

Cycle	Mode Based	Constant Fuel Cell	AECMS	Optimal
US06	50.58	49.50	49.23	50.00
HWFET	51.30	50.04	48.37	50.00
UDDS	49.70	49.16	49.92	50.00

Table 5.1: Simulation Final State of Charge (%)

Cycle	Mode Based	Constant Fuel Cell	AECMS	Optimal
US06	33.64	37.10	36.99	37.15
HWFET	58.33	63.15	65.00	63.86
UDDS	48.28	50.09	47.70	49.03

Table 5.2: Fuel Only Fuel Economy

Cycle	Mode Based	Constant Fuel Cell	AECMS	Optimal
US06	34.20	36.57	36.19	37.15
HWFET	61.14	63.25	61.46	63.86
UDDS	47.80	48.67	47.57	49.03

Table 5.3: Power Adjusted Fuel Economy

Cycle	Mode Based	Constant Fuel Cell	AECMS	Optimal
US06	34.19	36.58	36.21	37.15
HWFET	61.36	63.26	61.18	63.86
UDDS	47.72	48.44	47.55	49.03

Table 5.4: Optimal Charge/Discharge Fuel Economy

Cycle	Mode Based	Constant Fuel Cell	AECMS	Optimal
US06	34.19	36.58	36.21	37.15
HWFET	61.42	63.26	61.08	63.86
UDDS	47.61	48.13	47.52	49.03

Table 5.5: Averaged Charge/Discharge Fuel Economy

5.1.2 Drive Cycle Simulation Results

Plots of the simulation results for the fuel cell power, battery power and battery state of charge can be seen in Figures 5.1, 5.2, 5.3 and 5.4. The fuel economies for all simulations are captured in Tables 5.3, 5.4 and 5.5.

Optimal Simulation Results

The optimal solution, Figure 5.1, tends to have the fuel cell power, represented by the blue lines, follow very close to the average power demand of the drive cycle with only slight deviations to control the final battery state of charge. The three different drive cycles show drastically different power demands, represented by the red lines in Figure 5.1. Despite the drastic differences in the power demands, all three drive cycles have an average power demand that tends to fall within the 8 kW to 20 kW range. The 8 to 20 kW region happens to also closely match the fuel cell's 10 to 20 kW optimal operating region depicted in Figure 3.10. The average power demand coinciding with this region comes as a result of properly sizing the fuel cell for this particular type of vehicle. These results show that it is most efficient to run the fuel cell at near peak efficiency as much as possible and let the battery follow the net load.

Mode Based Control Simulation Results

The mode based strategy, Figure 5.2, shows a very different approach to controlling the vehicle. The fuel cell primarily follows the power demand with the battery supplementing the power demand and acting primarily as a buffer to handle transients. The mode based strategy continually switches between charging and discharging the battery based on the SOC without any direct regard for fuel cell efficiency, as shown by the sawtooth pattern in the SOC plots of all three drive cycles in Figure 5.2. The mode based strategy frequently drives the fuel cell's operating point outside the optimal operating region of the fuel cell which is shown in Figure 3.10.Running the fuel cell outside the 10 to 20 kW region cause the fuel cell to waste hydrogen which directly impacts the fuel economy. In the US06 cycle the fuel cell is frequently run above the 20 kW operating region. In the UDDS cycle, this strategy frequently idles the fuel cell bringing the operating point below 8 kW and wasting hydrogen since no usable energy is produced from the fuel cell at that time and all hydrogen consumed is used to keep the fuel cell active. Since the fuel cell has long start up and shut down times which take several minutes, it is not even practical to turn off the fuel cell during these brief but frequent idling periods. From the fuel economy results

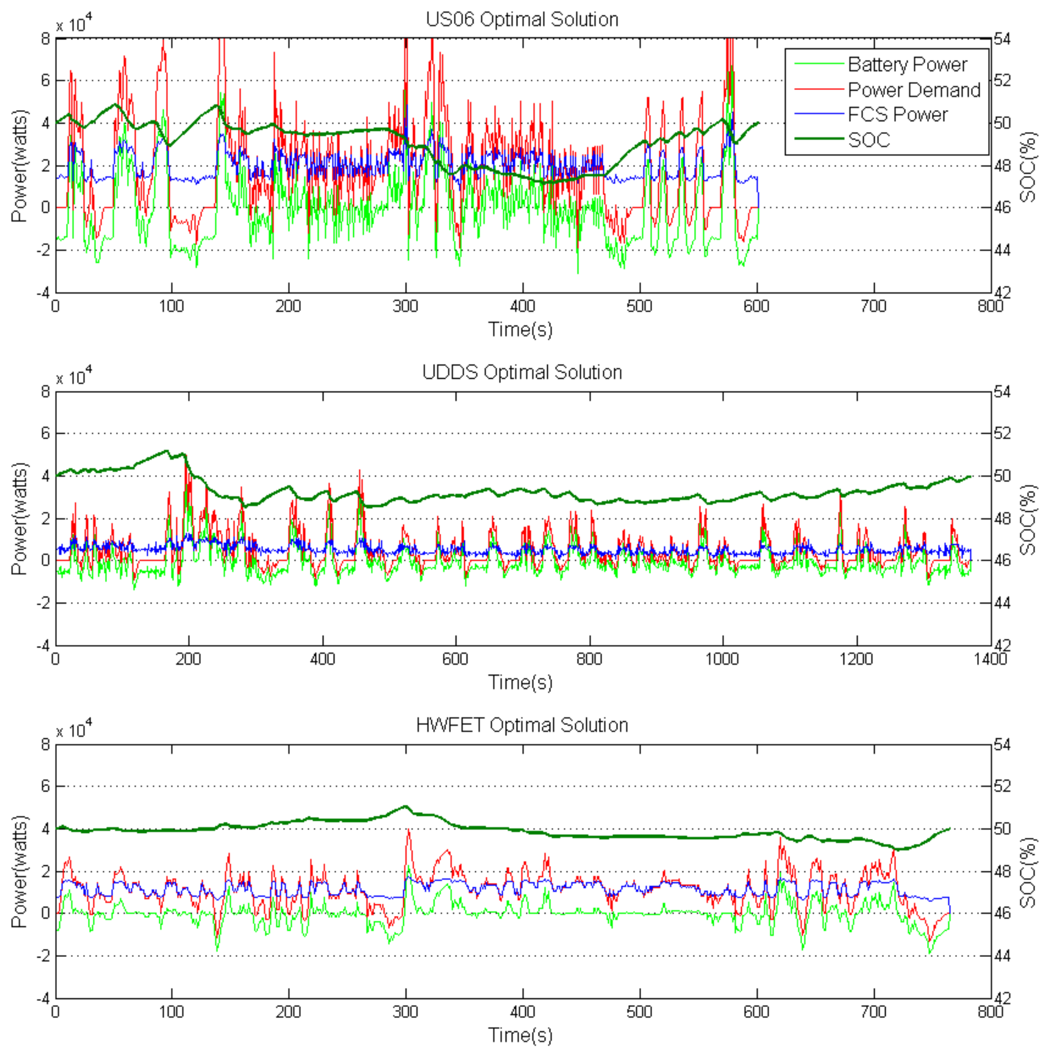

Figure 5.1: Optimal Solutions

in Tables 5.3, 5.4 and 5.5, it is apparent that the mode based strategy consistently shows the lowest fuel economy, which come as a result of the fuel cell running at much more inefficient operating points throughout the drive cycles.

Constant Fuel Cell Simulation Results

The constant fuel cell strategy, Figure 5.3, stands out from the rest of the controllers in that it is both easy to implement and provides the highest fuel economy numbers for an implementable controller. Despite the 150 A current limit of the DC/DC converter, this strategy was able to operate the fuel cell at the average power demand without any significant adjustments to the fuel cell power set point required to ensure that the system respects the component limits. The UDDS and HWFET drive cycles show consistently constant fuel cell power output plots while the US06 cycle shows some changes in the fuel cell set point at 150, 300 and 680 seconds to prevent the vehicle from exceeding the DC/DC converter current limit. These three adjustments are very brief and do not substantially impact the vehicle fuel consumption. Had the vehicle component limits been more severe, it is possible that this strategy may not have proven to be as effective. At the same time, the drive cycles tested do not include unusual driving patterns such as significant idle times and extremely aggressive driving which may have moved the average fuel cell operating point outside the optimal operating region and would have negatively impacted the fuel economy. The evaluation of the constant fuel cell strategy under these cases is left for future research. The constant fuel cell approach uses the fuel cell very efficiently for the tested drive cycles, but extensively uses the battery to satisfy power demand, resulting in additional losses through the DC/DC converter and potentially more significant wear on the battery system which may impact the battery life. Further research is needed to fully evaluate the impacts of this strategy on the life of the battery system. The additional efficiency losses through the DC/DC tend to be lower than the losses of operating the fuel cell inefficiently, which is why the constant fuel cell strategy has a such a good fuel economy.

A-ECMS Simulation Results

The A-ECMS strategy, Figure 5.4, shows a similar trace to the optimal solution. The main difference is that the average operating point of the fuel cell shifts throughout the drive cycle as the value of battery power changes in the cost function due to the adaptive elements of the controller. The gradual shifting of the power demand is visible in all three drive cycles and is evidenced by the curve of the blue fuel cell power output plot. There

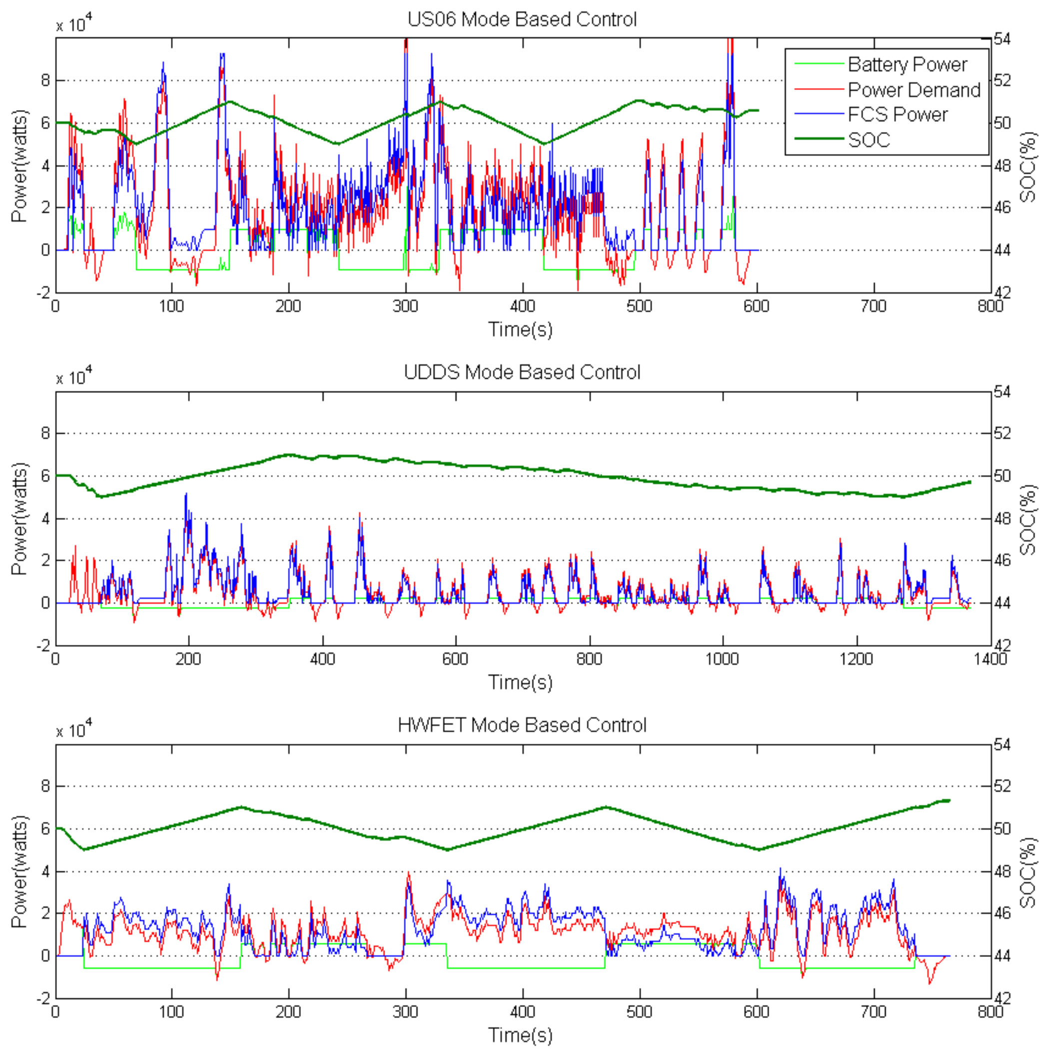

Figure 5.2: Mode Based Control Solutions

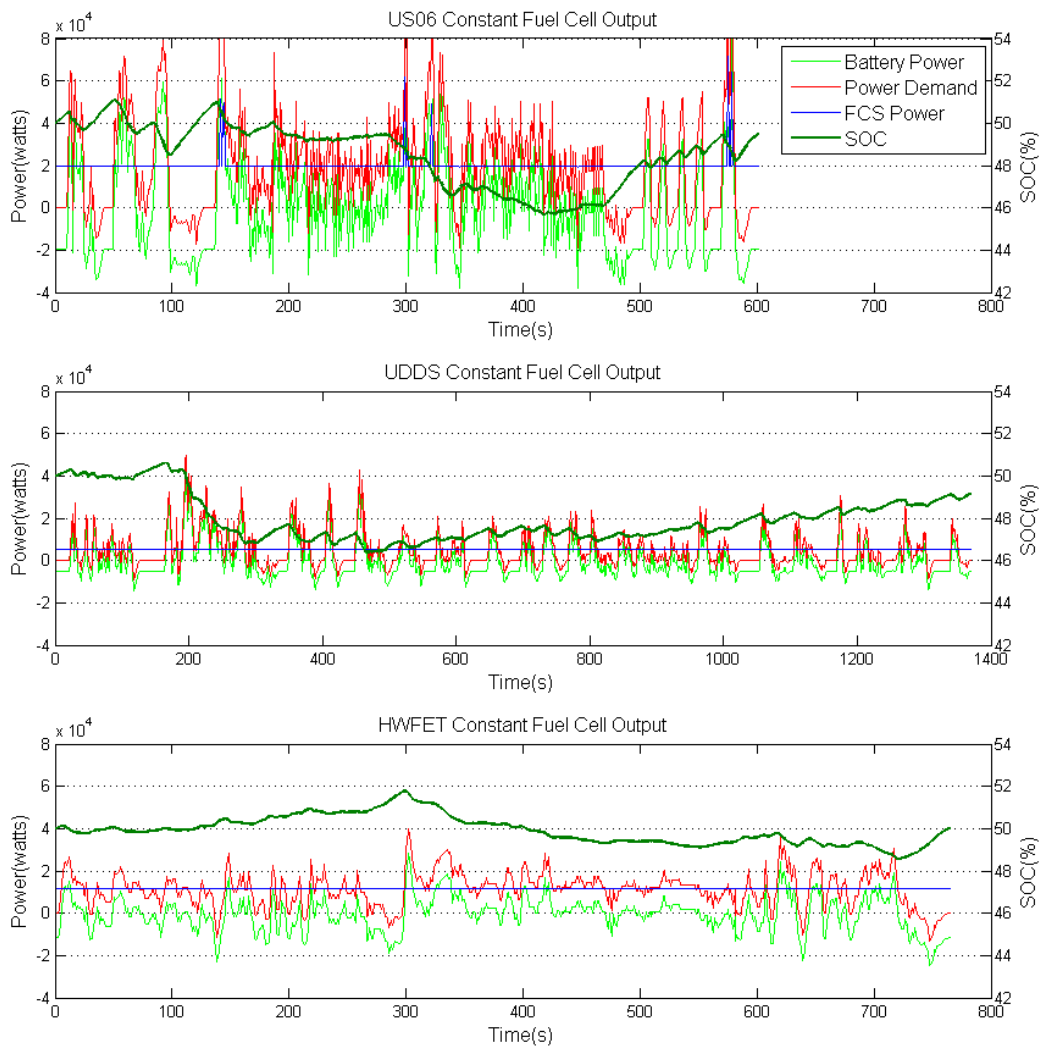

Figure 5.3: Constant Fuel Cell Output Solutions

are times where the A-ECMS strategy idles the fuel cell in the UDDS cycle, bringing the power output down to zero and negatively impacting the fuel economy. There is a notable trade off between adapting to changes in the power demand and trying to stay close to the 10 to 20 kW peak fuel cell efficiency region. Operating outside the 10 to 20 kW region and idling the fuel cell directly affects the efficiency of the solution and is the reason that the constant fuel cell strategy shows better results than the A-ECMS strategy.

5.2 Experimental Results

Experimental result were gathered from the vehicle using on-road testing for both the mode based and the constant fuel cell strategies. The poor performance of the A-ECMS strategy in simulation, coupled with the expanded implementation difficulty and limitations in the availability of hydrogen led for it to be discarded as a control strategy for on-road experimentation. To protect the vehicle hardware, both the tested strategies are wrapped in safety control logic designed to prevent the control logic from exceeding the power limits of the fuel cell, battery and DC/DC converter.

The goal of the on-road testing was to get a mix of urban and local highway style driving over a short drive cycle. Testing was done manually by maintaining constant vehicle speeds and performing uniform accelerations between defined markers. Test driving was done early in the morning on weekends at a time when there was very little traffic to ensure consistent driving conditions. Plots of two separate test runs are presented in Figure 5.5, and while the plots are close, small deviations do exist between runs. This is shown in more detail by examining a plot of the power demands for the two drive cycle runs which can be found in Figure 5.6. The power demands vary significantly at various times as a result of slightly different acceleration and braking patterns. Such variations are expected in on-road testing and, although not available to our team, a chassis dynamometer could be used to reduce the inter-cycle variation in subsequent testing. To ensure that these variations do not impact the results of the comparison, the optimal control strategies for both cycles have been independently determined. The experimental results are compared by evaluating the percentage of the optimal fuel economy achieved for the corresponding test cycle. The optimal solutions are configured so the final SOC is allowed to deviate by 1% of the final SOC of experimental results. This is to accommodate for the 0.5% resolution of the battery SOC reported by the battery controller which can account for up to 1% error in the SOC reported by the battery throughout the drive cycle. The averaged charge/discharge method has been used to measure the fuel economies.

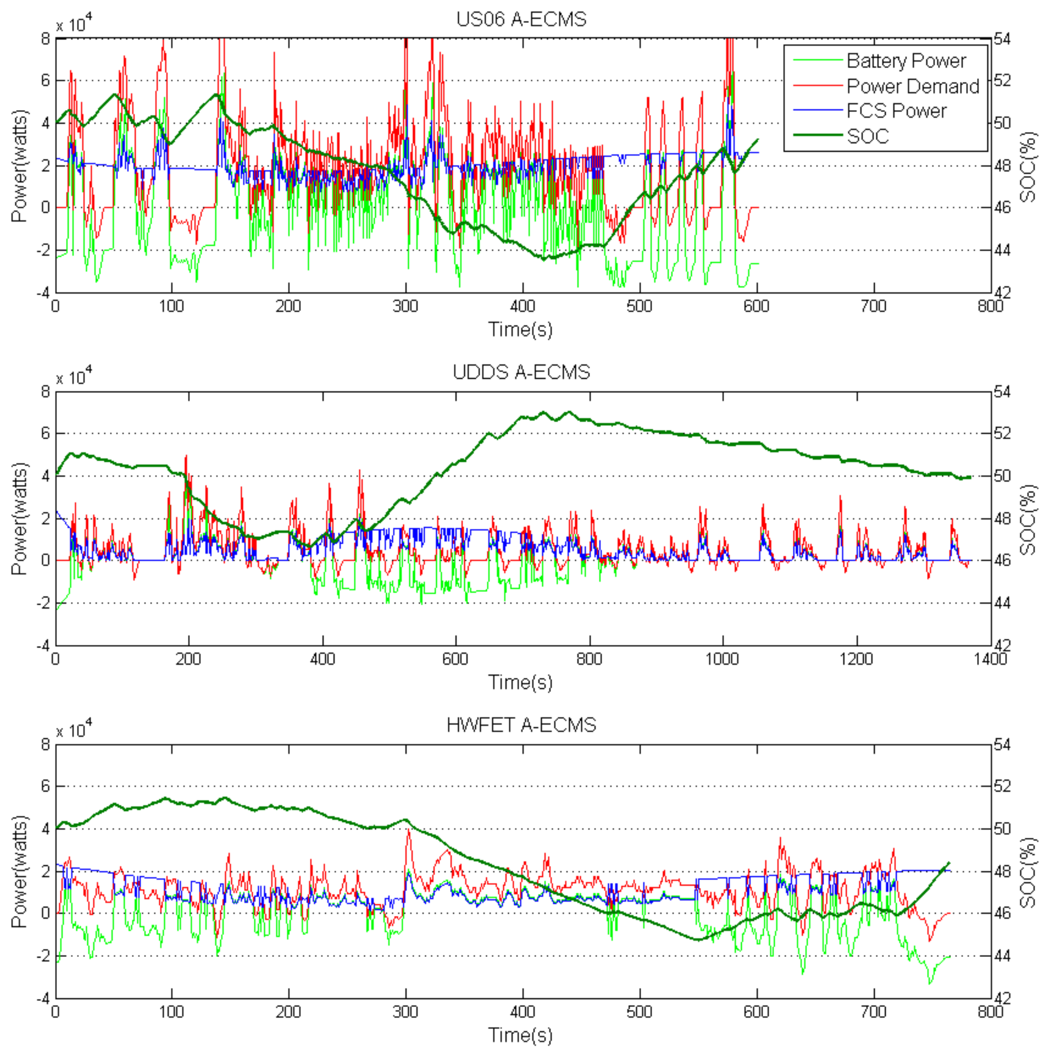

Figure 5.4: A-ECMS Solutions

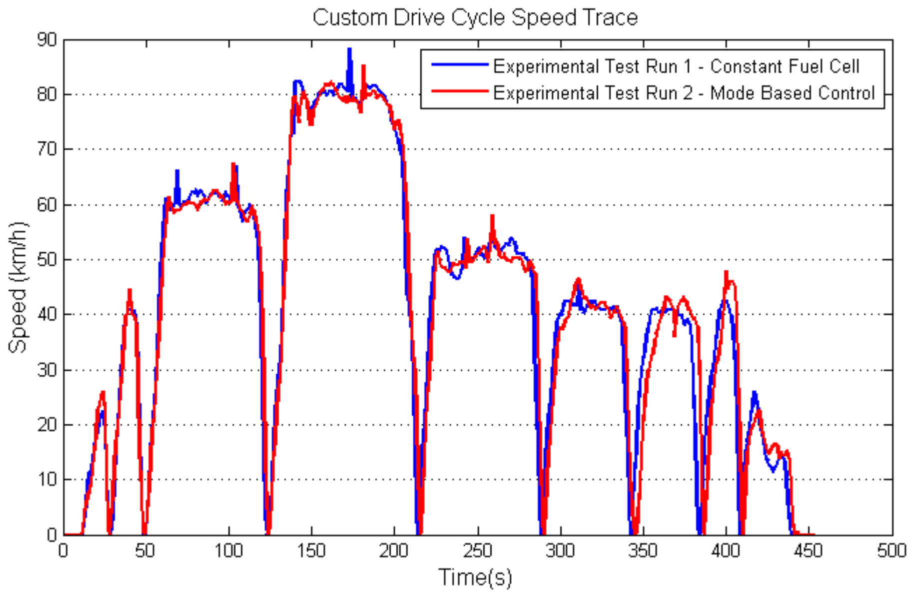

Figure 5.5: Custom Drive Cycle

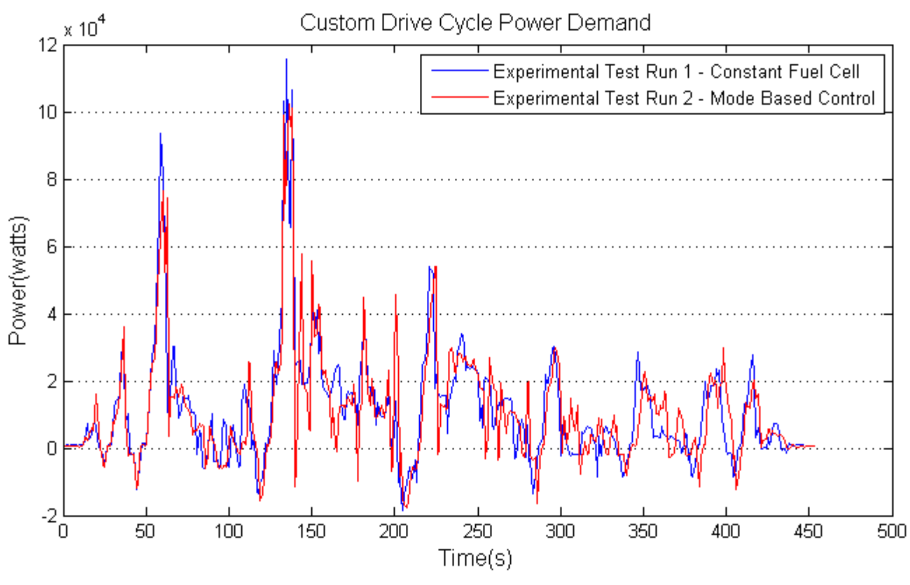

Figure 5.6: Custom Drive Cycle Power Demand

Control Strategy	Experimental Result	Optimal	Percentage of Optimal
Mode Based Control	31.60 mpg	33.30 mpg	94.89 %
Constant Fuel Cell	32.40 mpg	32.87 mpg	98.57 %

Table 5.6: Experimental Fuel Economy Results

5.2.1 Drive Cycle Experimental Results

Figure 5.7 presents the constant fuel cell strategy experimental results along with the corresponding optimal solution. Figure 5.8 presents the mode based control experimental results along with the optimal solution determined through simulation. Table 5.6 presents the fuel economies for these results. From Figures 5.7 and 5.8, it can be seen that the constant fuel cell strategy shows a very similar plot to the optimal solution. This is reflected in the fuel economy which is 98.57% of the optimal value. The deviations in the constant fuel cell solution are a result of the safety control logic designed to protect the major powertrain components. The mode based solution shows a slightly lower fuel economy which is 94.89% of the optimal. The plot of the mode based solution looks very similar to the optimal solution but more aggressively changes the power demand of the fuel cell to match the trace instead of using the battery to supplement the power demand. The constant fuel cell strategy shows a 4% improvement in fuel economy over the mode based control strategy.

The simulations and experiments showed consistent relative results, validating the fidelity of the simulations. Both the simulation and experimental results agree that a constant fuel cell strategy provides near optimal fuel economies for this vehicle configuration where the fuel cell has been sized properly for the average power demand expected during the vehicle's normal operation.

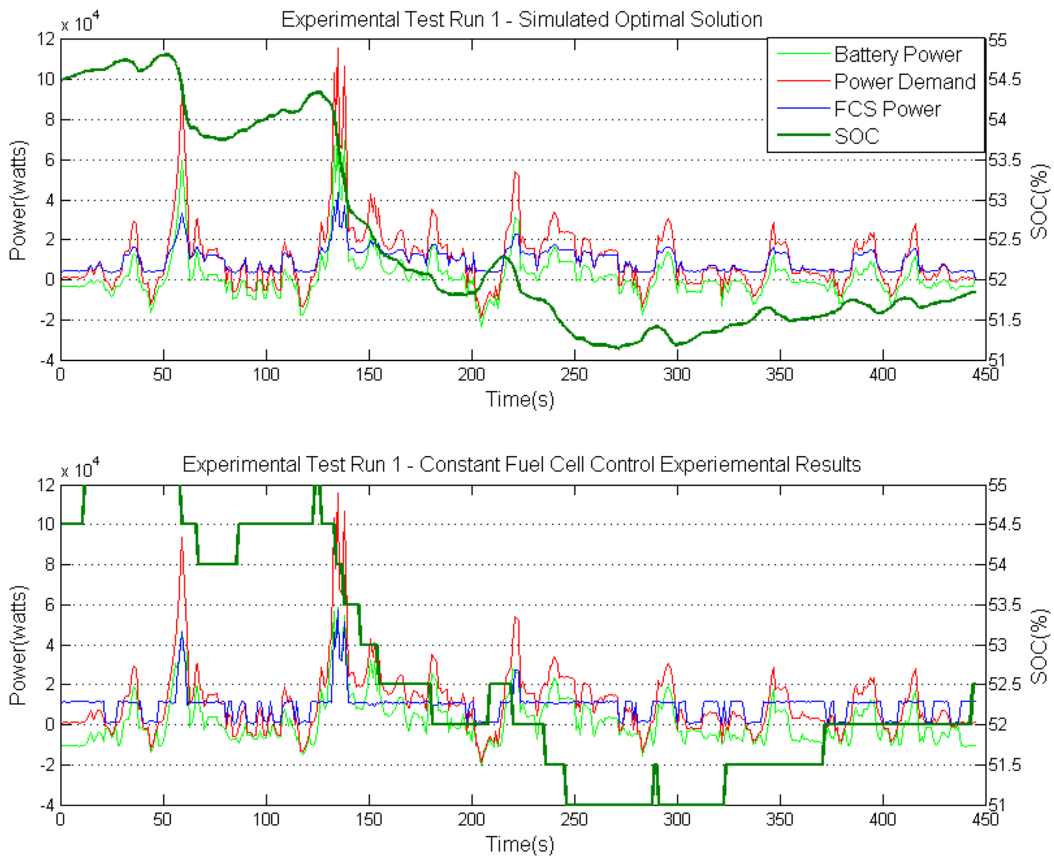

Figure 5.7: Experimental Test Run 1 - Constant Fuel Cell

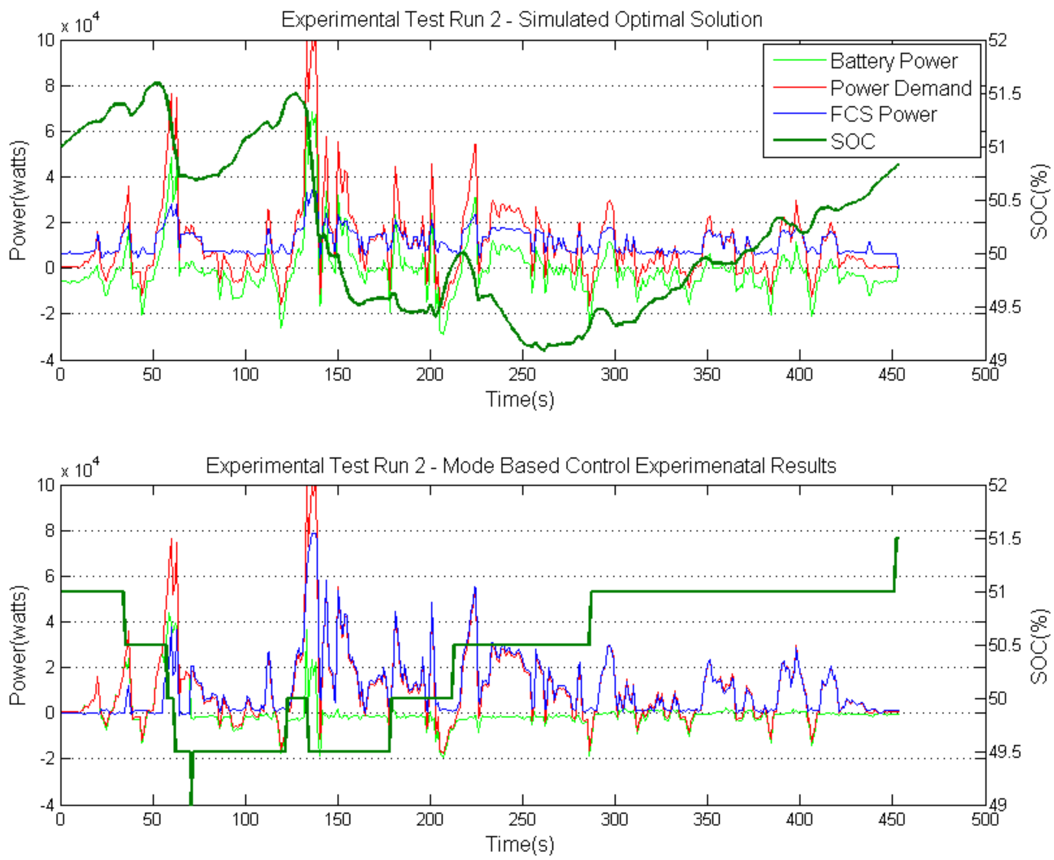

Figure 5.8: Experimental Test Run 2 - Mode Based Control

Chapter 6

Conclusion

With increasing concerns over the environmental impact of vehicles and reliance on depleting fossil fuels, hybrid vehicles are quickly becoming the new standard for vehicle design. To completely eliminate concerns over fossil fuel usage and the resulting harmful emissions the automotive industry is already looking towards the future of hybrid vehicle technology with hydrogen fuel cell powered hybrids. Fuel cell hybrids have numerous benefits over conventional hybrids including a higher efficiency energy production, environmentally friendly emissions and independence from fossil fuels. A substantial amount of research and development still needs to be done to make fuel cell hybrids viable for general consumer use. One such area of research is fuel cell hybrid vehicle control. Conventional hybrid vehicle control has been extensively studied by numerous researchers. Due to the relatively new development of road-safe fuel cell hybrids, most hybrid control theories have not yet been studied on passenger fuel cell powered vehicles.

This thesis has set out to fill in the gap in fuel cell hybrid vehicle control design by evaluating several common hybrid control strategies on a fuel cell hybrid vehicle. These strategies include an adaptive version of the popular equivalent consumption minimization strategy and two rule-based strategies; a constant fuel cell strategy which runs the fuel cell at a constant output, and a mode based strategy which switches operating modes based on changes in the battery state of charge and vehicle power demand. These strategies are implemented in simulation on a model of the vehicle powertrain developed in Matlab and then evaluated against optimal solutions determined by formulating the optimization problem as a quadratic programming problem.

6.1 Simulation Conclusions

The simulated results of the optimal solution showed that the best results can be achieved by closely tying the fuel cell power output to the peak efficiency operating points of the fuel cell. This is intuitively expected since the efficiency of the fuel cell changes very dramatically depending on the fuel cell operating point, as depicted in Figure 3.10, while the battery efficiency remains constant. Achieving the best possible fuel economy would therefore come as a result of minimizing efficiency losses in the fuel cell.

The constant fuel cell strategy takes advantage of this characteristic by keeping the fuel cell output at a constant high efficiency point which resulted in the constant fuel cell strategy producing the best fuel economies of all the tested strategies. The high fuel economy of the constant fuel cell strategy comes as a direct result of properly sizing the fuel cell for the vehicle which caused the average power demand of the vehicle to consistently be near the optimal efficiency operating region of the fuel cell. By properly sizing the fuel cell and running the fuel cell at the average power demand while using the battery to handle transients, the overall change in the battery state of charge is kept minimal while the fuel cell consistently operates near peak efficiency, producing very high fuel economy results for all the tested drive cycles.

The mode based strategy was originally used in the EcoCAR competition and was designed to reduce power flow through the DC/DC converter in order to protect the vehicle powertrain from exceeding current and voltage limitations. The mode based strategy shows a very different approach from the optimal strategy with the fuel cell directly following the power demand. The mode based strategy operates without any direct regard for fuel cell efficiency, often idling the fuel cell. As a direct result of consistently operating outside the high efficiency region for the fuel cell, this strategy shows the lowest fuel economy of all the tested strategies.

A-ECMS is an adaptive version of the equivalent consumption minimization strategy which was designed to take the fuel economy optimization problem and reduce it to an instantaneous optimization based on the fuel map of the engine and the battery state of charge. A-ECMS was originally developed for use on conventional hybrids. The research done as part of this thesis has adapted this strategy for use on hydrogen fuel cell hybrid vehicles.

The A-ECMS results show a plot that is similar to the constant fuel cell strategy but can periodically shift outside the optimal operating range of the fuel cell which negatively impacts the fuel economy. This strategy is far more sensitive to changes in the vehicle power demand than the constant fuel cell strategy which resulted in very poor traces for the UDDS cycle and ultimately lower fuel economy results.

6.2 Experimental Conclusions

To validate the simulation results, the mode switching and constant fuel cell strategies were evaluated on a fully operational fuel cell hybrid vehicle that was built by the University of Waterloo Alternative Fuels Team. The test vehicle was initially built for the EcoCAR competition and is based on a 2009 Saturn Vue which has been refit with two electric motors, a Li-ion battery and an automotive grade fuel cell system. A significant amount of work has been put into developing this vehicle. The A-ECMS was not implemented on the vehicle due to its complexity combined with the lower simulated fuel economy results and limitations in hydrogen availability.

Using the vehicle produced by the student team, the mode-based strategy and constant fuel cell strategy were tested on-road using a customized drive cycle that contained a mix of residential, local and highway driving conditions. During on-road testing, the drive cycles were found to have some minor variations. To account for these variations, the two strategies were compared by measuring their effectiveness compared to optimized results. The experimental results validated the simulation results with the constant fuel cell strategy providing notably better results that were much closer to the optimal solution. The results showed that the constant fuel cell strategy achieved a fuel economy which was within 98.57% of the optimal solution which demonstrates that this strategy is extremely effective for fuel cell based hybrid vehicles. One caveat is that in order for this strategy to be effective, it is necessary for the fuel cell to be sized properly for the vehicle's power demand so that the constant fuel cell power demand is near the peak efficiency point for the fuel cell.

6.3 Overall Conclusions

The research presented here has found that a simple practical strategy can produce very effective results for hybrid hydrogen fuel cell vehicles. The simulation results demonstrate that maintaining the fuel cell at a constant power output near its peak efficiency is the most effective means of reducing fuel consumption. Both the optimal solution and constant fuel cell strategy demonstrate this observation, and to a lesser extent, the A-ECMS strategy does as well. While the A-ECMS strategy shows reasonable results in simulation, the added complexity of this strategy does not make it practical for use in a fuel cell vehicle over the far simpler and more efficient constant fuel cell strategy. Further improvements to the A-ECMS which restrict the adaptation to a small band of operating points within the peak efficiency region of the fuel cell may improve the A-ECMS results. In its current form, the A-ECMS does not produce sufficiently good results to support its use in fuel cell powered vehicles. The mode based strategy used in the vehicle competition shows reasonable results but is consistently inferior to the more efficient constant fuel cell strategy. The simulation results are validated through on-road testing with a hybrid hydrogen fuel cell vehicle test bed. In on-road testing, the constant fuel cell strategy outperformed the mode based strategy by a similar margin to the simulations. By managing the fuel cell set point to control the battery state of charge, the constant fuel cell strategy can be used as a highly efficient yet simple control strategy for fuel cell vehicles.

6.4 Future Research

With the vehicle's fuel cell and hydrogen storage system removed, the University of Waterloo will be unable to continue fuel cell hybrid control research on this vehicle. If UWAFT decides to build another fuel cell vehicle in future competitions, the university will have the opportunity of evaluating these strategies on a different vehicle in order to validate that these results hold constant for other fuel cell vehicles.

Ideally, future research would also expand on the capabilities of the constant fuel cell strategy and consider variations of this strategy which allow for on/off operation of the fuel cell and more advanced methods of predicting the average power demand. Additional testing of this strategy should also be done under more unusual and aggressive drive cycles.

Additional research should also be done on charge depletion control strategies. Charge depletion strategies must take into account the distance to be driven and battery power available in order to determine the best control strategy as these factors directly impact the fuel economy of the vehicle in a far more substantial way than in charge sustaining control. The research discussed in this thesis focuses primarily on charge sustaining control strategies. There is still substantial room for studying charge depletion control as it relates to fuel cell powered vehicles. Future research would ideally focus on this area.

This work presents a viable set of controllers for fuel cell hybrids, with a clear winner in terms of ease of implementation and efficiency. Identifying the constant fuel cell controller and evaluating it on a real vehicle is an important step to enabling eventual deployment of fuel cell hybrids as commercially viable vehicles.

References

[1] History of hybrid vehicles. http://www.hybridcars.com/history/history-of-hybrid-vehicles.html. Accessed: Aug 2012.

[2] B. Blunier-D. Bouquain A. Ravey, N. Watrin and A. Miraoui. Energy-source-sizing methodology for hybrid fuel cell vehicles based on statistical description of driving cycles. *IEEE Transactions on Vehicular Technology*, 60(9):4164–4174, 2011.

[3] S. Pagerit A. Rousseau and D. Gao. Plug-in hybrid electric vehicle control strategy parameter optimization. *Journal of Asian Electric Vehicles*, 6(2):1125–1133, 2008.

[4] M. Back A. Sciarretta and L. Guzzella. Optimal control of parallel hybrid electric vehicles. *Control Systems Technology, IEEE Transactions on*, 12(3):352–363, 2004.

[5] M. Matian B. Wu and G. Offer. Hydrogen pemfc system for automotive applications. int. j. low-carbon tech. *International Journal of Low-Carbon Technologies*, 7(1):28–37, 2012.

[6] A. Biyikoglu. Review of proton exchange membrane fuel cell models. *International Journal of Hydrogen Energy*, 30:1181–1212, 2005.

[7] D. Boettner and M. Moran. Proton exchange membrane (pem) fuel cell-powered vehicle performance using direct-hydrogen fueling and on-board methanol reforming. *Journal of Energy Resources and Technology*, 29:2317–2330, 2004.

[8] H. Braun. The phoenix project: Shifting to a solar hydrogen economy by 2020. *Chemical Industry & Chemical Engineering Quarterly*, 14(2):107–118, 2008.

[9] K. Bhattacharya-M. Fowler M. Kazerani R. Fraser I. Rowlands C. Canizares, J. Nathwani and H. Gabbar. Towards an ontario action plan for plug-in-electric vehicles (pevs). Technical report, Waterloo Institute for Sustainable Energy, 2010.

[10] H. Peng C. Lin, M. Kim and J. Grizzle. System-level model and stochastic optimal control for a PEM fuel cell hybrid vehicle. *Journal of dynamic systems, measurement, and control*, 128:878–890, 2006.

[11] Y. Guezennec C. Musardo, G. Rizzoni and B. Staccia. A-ECMS: an adaptive algorithm for hybrid electric vehicle energy management. In *44th IEEE Conference on Decision and Control and the European Control Conference*, page 1816–1822, Seville, Spain, 2005.

[12] C. Chan. The state of the art of electric, hybrid, and fuel cell vehicles. *Proceedings of the IEEE*, 95(4):704–718, 2007.

[13] D. Cheddie and N. Munroe. Review and comparison of approaches to proton exchange membrane fuel cell modeling. *Journal of Power Sources*, 147:72–84, 2005.

[14] Y. Guezennec-G. Rizzoni D. Boettner, G. Paganelli and M. Moran. On-board reforming effects on the performance of proton exchange membrane (pem) fuel cell vehicles. *Journal of Energy Resources and Technology*, 124:191–196, 2002.

[15] Y. Guezennec-G. Rizzoni D. Boettner, G. Paganelli and M. Moran. Proton exchange membrane fuel cell system model for automotive vehicle simulation and control. *Journal of Energy Resources and Technology*, 124:20–27, 2002.

[16] S. Pagerit D. Karbowski, A. Rousseau and P. Sharer. Plug-in vehicle control strategy: from global optimization to real time application. In *22nd Electric Vehicle Symposium, EVS22, Yokohama, Japan*, 2006.

[17] C. Hsu F. Weng and C. Li. Experimental investigation of pem fuel cell aging under current cycling using segmented fuel cell. *International Journal of Hydrogen Energy*, 35(8):3664–3675, 2010.

[18] J. Baschuk G. Karimi and X. Li. Performance analysis and optimization of pem fuel cell stacks using flow network approach. *Journal of Power Sources*, 147:162–177, 2005.

[19] L. Guzzella and A. Sciarretta. *Vehicle propulsion systems: introduction to modeling and optimization*. Springer Verlag, Berlin Heidelberg, 2005.

[20] S. Anwar H. Banvait and Y. Chen. A rule-based energy management strategy for plug-in hybrid electric vehicle (PHEV). In *AACC American Control Conference*, page 3938–3943, St. Louis, MO, 2009.

[21] S. Anwar H. Banvait, X. Lin and Y. Chen. Plug-in hybrid electric vehicle energy management system using particle swarm optimization. In *EVS24 International Battery, Hybrid and Fuel Cell Electric Vehicle Symposium*, Stavanger, Norway, 2009.

[22] G. Jian-ping H. Hong-wen and Z. Ya-ming. Fuel cell output power-oriented control for a fuel cell hybrid electric vehicle. In *AACC American Control Conference*, page 605–610, Seattle, WA, 2008.

[23] K. Haraldsson and K. Wipke. Evaluating pem fuel cell system models. *Journal of Power Sources*, 126:88–97, 2004.

[24] H. Peng J. Pukrushpan and A. Stefanopoulou. Control-oriented modeling and analysis for automotive fuel cell systems. *Journal of Dynamic Systems Measurement and Control*, 126:14–25, 2004.

[25] Y. Park J. Ryu and M. Sunwoo. Electric powertrain modeling of a fuel cell hybrid electric vehicle and development of a power distribution algorithm based on driving mode recognition. *Journal of Power Sources*, 195(17):5735–5748, 2010.

[26] J. Martin-H. Wang J. Zhang J. Wu, X. Yuan and J. Shen. A review of pem fuel cell durability: degradation mechanism, mitigation strategies, and modeling. *Journal of Power Sources*, 184(1):104–119, 2008.

[27] H. Louahlia-Gualous L. Dumercy, R. Glises and J. Kauffmann. Thermal management of a pemfc stack by 3d nodal modeling. *Journal of Power Sources*, 156:78–84, 2006.

[28] S. Onori L. Serrao and G. Rizzoni. A comparative analysis of energy management strategies for hybrid electric vehicles. *Journal of Dynamic Systems, Measurement and Control, Transactions of the ASME*, 133(3), 2011.

[29] X. Li. *Principles of Fuel Cells.* Taylor & Francis, New York, NY, 1st edition, 2006.

[30] Y. Gao M. Ehsani and A. Emadi. *Modern Electric, Hybrid Electric, and Fuel Cell Vehicles: Fundamentals, Theory, and Design, Second Edition.* CRC Press, Boca Raton, FL, September 2009.

[31] B. de Jager W. Heemels P. Van den Bosch M. Koot, J. Kessels and M. Steinbuch. Energy management strategies for vehicular electric power systems. *Vehicular Technology, IEEE Transactions on*, 54(3):771–782, 2005.

[32] B. Surgenor M. Mallouh, M. Al-Marouf and B. Peppley. Effect of control strategy on the performance of a fuel cell hybrid electric auto rickshaw. Technical Report 2011-01-1174, SAE International, Warrendale, PA, April 2011.

[33] J. Mierlo and G. Maggetto. Fuel cell or battery: Electric cars are the future. *Fuel Cells*, 7(2):165–173, 2007.

[34] J. Miller. *Propulsion Systems for Hybrid Vehicles*. IET, 2004.

[35] B. Blunier N. Watrin and A. Miraoui. Review of adaptive systems for lithium batteries state-of-charge and state-of-health estimation. In *IEEE Transportation Electrification Conference and Expo*, 2012.

[36] B. Blunier N. Watrin, D. Bouquain and A. Miraoui. Multiphysical lithium-based battery pack modeling for simulation purposes. In *IEEE Vehicle Power and Propulsion Conference*, 2011.

[37] The National Hydrogen Association. *The Energy Evolution: an analysis of alternative vehicles and fuels to 2100*, 2009.

[38] A. Priddle. Toyota to start selling hydrogen fuel-cell car in 2015. *USA Today*, 2012. http://content.usatoday.com/communities/driveon/post/2012/08/toyota-to-start-selling-hydrogen-fuel-cell-car-in-2015/1. Accessed: Sept 2012.

[39] R. Carlson Q. Cao, S. Pagerit and A. Rousseau. PHEV hymotion prius model validation and control improvements. In *EVS23 International Electric Vehicle Symposium*, Anaheim, CA, 2007.

[40] Y. Li Q. Gong and Z. Peng. Optimal power management of plug-in HEV with intelligent transportation system. In *Advanced intelligent mechatronics, 2007 IEEE/ASME international conference on*, page 1–6, Zurich, Switzerland, 2007.

[41] D. Xuan Q. Ning and Y. Kim. Modeling and control strategy development for fuel cell hybrid vehicles. *International Journal of Automotive Technology*, 11(2):229–238, 2010.

[42] A. Rousseau R. Ahluwalia, X. Wang and R. Kumar. Fuel economy of hydrogen fuel cell vehicles. *Journal of Power Sources*, 130:192–201, 2004.

[43] Y. Hou R. Lin, B. Li and J. Ma. Investigation of dynamic driving cycle effect on performance degradation and micro-structure change of pem fuel cell. *International Journal of Hydrogen Energy*, 34(5):2369–2376, 2009.

[44] C. Miulli S. Barsali and A. Possenti. A control strategy to minimize fuel consumption of series hybrid electric vehicles. *Energy Conversion, IEEE Transactions on*, 19(1):187–195, 2004.

[45] T. Guerra S. Delprat, J. Lauber and J. Rimaux. Control of a parallel hybrid powertrain: optimal control. *Vehicular Technology, IEEE Transactions on*, 53(3):872–881, 2004.

[46] J. Lee S. Lee, J. Kim and B. Cho. State-of-charge and capacity estimation of lithium-ion battery using a new open-circuit voltage versus state-of-charge. *Journal of Power Sources*, 185(1):1367–1373, 2008.

[47] J. Hin H. Wang K. Friedrich S. Zhang, X. Yuan and M. Schulze. A review of platinum-based catalyst layer degredation in proton exchange membrane fuel cells. *Journal of Power Sources*, 194(1):588–600, 2009.

[48] A. Sciarretta and L. Guzzella. Control of hybrid electric vehicles. *Control Systems Magazine, IEEE*, 27(2):60–70, 2007.

[49] M. Stevens. *Hybrid Fuel Cell Vehicle Powertrain Development Considering Power Source Degradation*. PhD thesis, University of Waterloo, 2008.

[50] O. Sundstrom and A. Stefanopoulou. Optimum battery size for fuel cell hybrid electric vehicle - part i. *Journal of Fuel Cell Science and Technology*, 4:167–175, 2007.

[51] E. Tate and S. Boyd. Finding ultimate limits of performance for hybrid electric vehicles. *SAE Transactions*, 109(6):2437–2448, 2000.

[52] C. Thomas. Comparison of transportation options in a carbon-constrained world: Hydrogen, plug-in hybrids and biofuels. Technical report, National Hydrogen Association Annual Meeting, 2008.

[53] UWAFT. University of waterloo alternative fuels team. http://uwaft.com/. Accessed: Aug 2012.

[54] C. Winter. Hydrogen energy - abundant, efficient, clean: A debate over the energy-system-of-change. *International Journal of Hydrogen Energy*, 34:S1–S52, 2009.

[55] J. Wen X. Wu, B. Cao and Y. Bian. Particle swarm optimization for plug-in hybrid electric vehicle control strategy parameter. In *IEEE Vehicle Power and Propulsion Conference*, page 1–5, Harbin, China, 2008.

[56] H. Wang J. Wu J. Sun R. Hiesgen K. Friedrich M. Schulze X. Yuan, S. Zhang and A. Haug. Degradation of a polymer exchange membrane fuel cell stack with nafion membranes of different thicknesses: Part i. in situ diagnosis. *Journal of Power Sources*, 195(1):7594–7599, 2010.